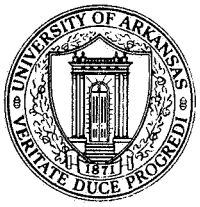

UNIVERSITY OF ARKANSAS

Graduate Institute of Technology

Department of Electronics and Instrumentation
Research Grant NsG 713
(NGR 04-001-007)

National Aeronautics and Space Administration
September 30, 1968

Informal Status Progress Report

for

NASA Research Grant NsG 713
(NGR 04-001-007)

for the period ending

September 30, 1968

INVESTIGATION OF LASER PROPERTIES RELEVANT TO THE MEASUREMENT OF DIFFERENT PHYSICAL PARAMETERS

Department of Electronics and Instrumentation

University of Arkansas Graduate Institute of Technology

Little Rock

M. K. Testerman
Principal Investigator

TABLE OF CONTENTS

I. DOUBLE EXPOSURE HOLOGRAPHIC INTERFEROMETRY WITH SEPARATE REFERENCE BEAMS

G. S. Ballard

Introduction:

A widely used method of holographic interferometry is the double exposure technique (1, 2, 3, 4). If two sets of waves are recorded on the same hologram by means of a double exposure, these waves will be reconstructed simultaneously and their resulting interference can be observed. The advantages of obtaining interferograms in this manner are well known. Precise optical components are not required, the displacement of diffuse surfaces can be observed, and the technique is well suited to the recording of transient phenomena by utilizing a pulsed laser to form the hologram.

The usual method of obtaining a double exposure hologram for interferometric studies is to change only the test scene between exposures. The same reference beam is used throughout. This results in an arrangement which is no more complex than that required to record and reconstruct any hologram made with an off-axis reference beam. One disadvantage of this method is that the reconstructions of the test scene and the comparison beam are inseparable, being linked together by the common reference beam. The particular interferogram presentation which is obtained is determined by the conditions present during the exposures and cannot be changed by the observer. The interferogram may not show the desired features of the test scene to the best advantage, possibly a serious problem when recording transient phenomena.

With the addition of several components, a typical off-axis hologram

arrangement can be modified into a three-beam system consisting of a single object beam and two different reference beams. This would permit a typical dual exposure hologram to be recorded, except that now a different reference beam can be used for each of the two exposures, allowing the test scene and the comparison beam to be reconstructed independently.

Various adjustments can be made between the two reconstructed beams, allowing many different interferometric presentations to be obtained from a single hologram. A small change in the angle of one of the reconstructing beams can cause either a zero order or a finite fringe interferogram to be observed. A phase shift induced in one of the reconstructing beams results in a relative phase shift between the two reconstructed beams, allowing the observed fringes to be displayed to the best advantage.

In addition, this method may prove useful in the investigation of transient phenomena which result in less than a single fringe being produced. In such an application, the comparison beam and an undisturbed portion of the test scene may be adjusted to possess a desired phase relationship. The relative phase of any portion of the test scene may now be determined by carefully measuring the shift necessary to bring the comparison beam into the desired phase relationship with that portion of the test scene being examined.

Work Performed

Several holograms have been recorded using the separate reference beam method. Figure 1 illustrates the arrangement of the components used. The test scene was recorded using beam R_1 as a reference. A stop was placed in beam R_2 so that it did not illuminate the recording medium. The test

object was then removed and the comparison beam was recorded in the same manner, except that beam R_2 was used as the reference and beam R_1 was stopped. The two reference angles, θ_1 and θ_2, must be selected so that unwanted reconstructed orders do not overlap the desired reconstruction.

After processing, the hologram was replaced in its original position. If it is illuminated by beam R_1 alone, the original test scene beam is reconstructed. If R_2 alone is used, the comparison beam is re-formed. Illumination by both R_1 and R_2 simultaneously reconstructs both the test scene and comparison beams, and an interferogram is observed. Some alignment of the hologram and the two reference beams may be necessary to obtain a zero order interferogram. In practice, this alignment has not proved difficult when parallel light is used to form the reference beams. The angle between the reconstructing beams can readily be adjusted until the two reconstructions are coincident. The use of spherical wavefronts to form the reference beams, however, adds the problem that any discrepency in the distance from the hologram to either reconstructing source will result in the formation of circular fringes, making alignment most difficult.

The test object used in these experiments was a microscope slide which produced an interesting fringe pattern. The holograms were recorded on Kodak 649-F glass plates. Since the hologram must be precisely aligned during reconstruction, the glass plates are preferable to a film substrate. Figures 2 through 5 show several of the presentations which can be obtained from a single hologram. In Figure 2, the two reconstructing beams have been aligned to result in a zero order interferogram of the subject. In Figure 3, the phase of the reconstructed comparison beam has been shifted

approximately 180 degrees with respect to the reconstructed test scene by inserting a proper thickness of glass in beam R_2 before collimation. Figure 3 also illustrates that phase shifts between the two reconstructed beams may result in some details of the test scene, which were not apparent, becoming more noticeable. Finite fringe interferograms are also obtainable from the hologram. A horizontal change in the angle of one of the reconstructing beams produced the vertical finite fringes of Figure 4. Similarly, a vertical change in the reconstructing angle gave the horizontal finite fringe interferogram in Figure 5. The orientation of the finite fringes as well as their spacing can be varied to any desired degree by a suitable movement of one of the reconstructing beams.

The hologram used to obtain the interferograms shown in the Figures was of a transparent object directly illuminated by the collimated laser beam. Interferograms have also been obtained from holograms in which the object was illuminated with diffuse light, with similar results.

In addition to the flexibility of presentation which has been demonstrated, this method of recording holographic interferograms should prove useful in evaluating interferograms of transient phenomena which result in less than a single fringe being observed. One technique for evaluating these interferograms can be explained as follows. Let us consider some small area of the interferogram, perhaps near the edge where the test scene has not been altered by the disturbance under study. If we place a photodetector at this location and illuminate the hologram with beam R_1 alone, the photodetector will give a signal proportional to the local intensity of the reconstructed test scene. This is represented by I_t in Figure 6. If now we were

to block off beam R_1 and illuminate the hologram with R_2 alone, our detector would give a signal proportional to the intensity of the reconstructed comparison beam at the same point. This is represented by I_c in Figure 6. If we now illuminate the hologram with both beams R_1 and R_2, the intensity of light at our detector will depend upon the relative phase of the two reconstructed beams. This phase dependent intensity is represented by I_s in Figure 6. If we now insert a chopper in beam R_1 at a convenient place prior to collimation, the output of our detector should be a square wave, as it sees only the comparison beam and then both beams together. The frequency of the signal would be determined by the chopping rate, and its amplitude would depend upon the relative phase of the two beams. Since the relative phase of these beams can be varied by the observer, it would be possible to adjust the relative phase until ϕ_n in Figure 6 is reached. At this point, the a-c output of the detector will be nulled out as there is no difference between the two intensities being detected. Rather than using a thickness of glass such as was utilized to obtain Figures 2 and 3, a small cell could be constructed wherein the index of refraction of the cell could be varied by changing the air pressure inside the cell. The cell pressure necessary to null the detector signal would be recorded. Now our detector can be moved to an area of interest in the interferogram. The detector signal at this point can be nulled in the same manner as was done before. If this null occurs at the same pressure as the previous point, it will mean that the two test points are in phase. If the two points are not in phase the pressure will be different. This difference in pressure will be a measure of the phase difference between the two points in the test scene.

In order to evaluate this technique, a test hologram was reconstructed as shown in Figure 7. The phase shifting cell consisted of a 3/4 inch aluminum plate through which a 1 inch hole had been drilled. Windows were attached to both sides of the plate, forming a chamber 3/4 inch thick. Provision was made to vary the pressure inside the cell by small amounts above and below atmospheric. The pressure inside the chamber was measured by means of a manometer utilizing dibutyl phthialate as a liquid. It was determined experimentally that a pressure change of 120 centimeters of manometer fluid was required to change the relative phase of the two reconstructed beams 360 degrees with the particular chamber thickness used. Thus, each centimeter change of pressure in the chamber corresponds to a phase shift of 1/120 of a fringe.

By repeatedly measuring the pressure required to null the signal at one particular point in the test beam, it was found that there was a phase drift between the two beams other than that introduced by the observer. This drift was apparently due to very slight changes in the optical path lengths of the two reconstructing beams caused by temperature changes. The normal drift between readings was approximately 2 centimeters of fluid, or about 1/60 of a wavelength. This drift prevented pressure readings from being reproduced and was the factor that limited the accuracy of the measurements. Even so, with only the original techniques and equipment used, phase changes to the nearest 1/60 of a fringe could be measured. Refinements in this technique or an improved method would certainly increase the sensitivity of the measurements.

Conclusions:

The separate reference beam method of recording dual exposure holographic interferograms possesses all of the advantages of the standard single reference beam technique while retaining the flexibility normally associated with a conventional real time interferometer. This method makes it possible to record interferograms of transient events holographically and then display the recorded information in the most advantageous manner.

With holograms made in this manner, it is possible to obtain information concerning the phase shifts in a field where only minute changes are found. A method has been investigated where phase changes of approximately 1/60 of a fringe can be measured. Improved methods will result in smaller phase shifts being accurately measured.

Future Work

Recording and reconstructing interferograms from separate reference beam holograms is now a routine procedure. However, the potential use of this type hologram to measure very small phase shifts in transient fields has only been demonstrated. As a first attempt, phase shifts as small as 1/60 of a wavelength can be measured. Future work will be aimed at improving the sensitivity and accuracy of these phase measurements. The present method can be improved by merely taking faster measurements. This would allow the interferometer less time in which to drift. Elimination of the drift or compensation for it would be a great improvement. All of the components of the system must be evaluated and the best combination selected. An entirely different method of readout will be investigated, wherein the phase difference between two points can be directly measured. This technique will require two detectors, but would eliminate the problem of phase drift and may prove the most advantageous.

II. THE SIMULATION OF ANALOG TRANSMISSION LOSSES

B. J. Harrell and G. S. Ballard

Introduction:

When a hologram is transmitted in an analog manner, one of the factors which will degrade the image obtained from the hologram as received is the attenuation of some of the higher hologram frequencies, caused by a limited time-bandwidth product. The effect of the loss of these higher frequencies was discussed in the NsG 713 progress report of December 31, 1967.

Another source of image degradation is transmission noise which is within the bandwidth required for the transmission of the holographic information. Since this noise cannot be filtered out of the signal, its effect upon the reconstructed holographic image must be ascertained. A study of the image degradation caused by such noise is the subject of this report.

The simulation of a noisy hologram was achieved in the following steps. A single hologram of a given object was recorded and used in all of the experiments. Several noise plates were made by exposing a photographic emulsion to a laser speckel pattern which contained random spatial frequencies within the same bandwidth as those contained within the hologram. The noise plates were identical except for their exposure times, the contrast of the plates being equivalent to the noise amplitude. A power spectrum was then obtained for each of the noise plates and for the hologram. From the spectral data, the relative amplitudes of "signal" from the hologram and "noise" from the noise plates were obtained. The hologram was then reconstructed with each

of the noise plates interposed, and the images obtained were evaluated by obtaining the modulation transfer function of each image. It could then be shown how the image was degraded for each of the different noise levels.

Work Performed

The hologram used to simulate the signal to be transmitted was recorded in the conventional manner, using an off-axis reference beam of parallel light. The object was a transparent National Bureau of Standards Resolution Chart which was illuminated from behind with diffuse light. The resolution chart consists of sets of lines of various spacings, and images of the chart are well suited for studies of image degradation. The hologram was recorded on a Kodak 649-F glass plate. The maximum and minimum angles between object and reference beams were determined by the recording geometry, and from these angles it was calculated that the spatial frequencies contained in the hologram covered a range of from 120 to 504 lines per millimeter. These lines represent the band of frequencies to be transmitted.

It was now desired to produce noise plates which contained random spatial frequencies within the same band as those frequencies found within the hologram. These noise plates were recorded as shown in Figure 8. The laser beam was expanded and collimated, giving a parallel beam four inches in diameter. This beam illuminated a sheet of frosted glass and became scattered, producing the characteristic laser "speckel pattern". The speckel pattern is known to contain spatial frequencies up to a maximum determined by the angle θ. The film plate was placed a distance D of 10 inches from the frosted glass, giving tan θ a value of 0.400 and sine θ a value of 0.371. Using the formula

$$f = \sin \theta / \lambda$$

we find the maximum spatial frequency recorded in the film plate to be 586 lines

per millimeter for the given value of sine θ and a wavelength λ of 6328 Angstroms. Thus, the noise plate meets the requirement of containing random spatial frequencies over the same range as those contained in the hologram.

So that a number of different noise levels could be simulated, several noise plates were made which were identical except that the exposure was varied from plate to plate. The noise plates eventually used in the experiment were exposed for periods of 1, 2, 3, and 4 seconds, and will be referred to as plate number 1, plate number 2, etc. respectively.

A power spectrum was made of the hologram and of each noise plate using the apparatus and methods described in Section III of this report. From this spectrum it was possible to obtain the signal level from the hologram and the noise levels of each of the noise plates for any desired frequency. It was decided to measure the signal/noise levels at a single frequency within the hologram band. The data obtained from a single frequency should give results consistent with those obtained if all of the individual frequencies were considered. A diffraction angle of 8.75 degrees, equivalent to a spatial frequency of 240 lines per millimeter, was chosen as being representative of all the frequencies present within the band of the hologram and the noise plates. A photomultiplier was used to detect the light diffracted by the hologram and noise plates at the desired angle. A voltage was read as the output of the photomultiplier, this voltage being proportional to the intensity of the light diffracted at the chosen angle. Since the optical density of each of the plates varied with exposure, the data as observed is not indicative of the true proportion of light diffracted by each plate. We would expect the observed noise from plate 4 to be significantly lower than that of the

other plates simply because it is more nearly opaque. Thus, in order to compare the light intensity observed for each plate, we must normalize the data. This can be accomplished by finding the ratio of the observed intensity at the chosen angle to the total intensity of light which passes through the plate. This light consists of transmitted light, diffracted light, and scattered light. Since by far the greatest portion of the light was transmitted directly through the plate, only the transmitted light was considered. The observed intensities, normalization factors, and normalized intensities are listed in Table 1.

Signal/noise ratios are usually calculated on the basis of amplitudes, so the intensity measurements for the plates were converted to amplitudes by finding their square roots. The ratio of hologram amplitude to noise plate amplitude at the angle of interest would give the signal/noise ratio upon reconstruction with a noise plate interposed in the reconstructing beam.

The actual noise present in transmitting a hologram will be determined by a number of factors. One of these is the method used for scanning the hologram. If the scan is horizontal, the unfiltered noise will cause unwanted light or "noise" to be diffracted horizontally and fall upon the image. In this case, the signal/noise ratio as described above is representative of this condition and is referred to as the "horizontal signal/noise". If, however, the transmitted noise is of random frequencies and random orientations, some very interesting observations result.

The noise plates as constructed for this experiment contain random frequencies with random orientations. Thus, in order to find the total noise present in the noise plate for a given frequency it is necessary to multiply the observed noise amplitude by $2\pi r$, where r is the distance from the zero

order transmitted light to that location in the Fourier plane at which the light diffracted by a given noise frequency appears. The radius r increases with spatial frequency.

The spatial frequencies within the hologram are oriented so that they diffract the incident light preferentially to one of the side orders associated with either the real image reconstruction or the virtual image reconstruction. Thus, in order to find the total signal present at a given frequency, it is not necessary to multiply by $2\pi r$ as was done for the noise plates, but by $2Ar$, where A is the angle formed by the upper and lower extremities of the signal in the Fourier plane with the transmitted zero order light (Figure 9). For the hologram used here, A = 0.053 radians. The factor of 2 arises from a need to consider both the real and virtual images, which are on opposite sides of the Fourier plane, as signal information. When these factors are taken into consideration, it can be seen that the signal/noise ratio declines to a lower value (Table 1). This ratio is referred to as the "total signal/noise".

After the signal/noise ratios had been determined for each of the four hologram-noise plate combinations, the hologram image was reconstructed with each of the noise plates interposed in the reconstructing beam. The "noisy" image was recorded on high contrast copy film. An image with the hologram alone was recorded to be used as a standard. These recorded images were placed on a microdensitometer and the Modulation Transfer Function obtained for resolved image lines. The MTF better describes the image quality of a system than the resolution limit. The MTF can assume values ranging from 0 to 1.0, and is evaluated by

$$MTF = \frac{E_{max} - E_{min}}{E_{max} + E_{min}}$$

where E_{max} and E_{min} are the maximum and minimum of the sine response recorded by a densitometer scan of a resolution chart image. It was observed that it was very difficult to obtain meaningful MTF's for the various recorded images. The main problem encountered was in focusing the reconstructed real image precisely on the recording film. The lines resolved in the image were spaced so closely as to make focusing difficult. This was complicated by the fact that the hologram used had a large aperture and was made with diffuse illumination. These two parameters contribute to a very limited depth of focus, and a small movement of the camera resulted in a serious degradation of the image. In order to obtain the best possible image from each hologram-noise plate combination, a number of exposures were made of each image. The camera was moved a small increment between each exposure, and the best image was chosen for evaluation. Even so, some discrepancies in this data are obvious.

The MTF's for each of the four noise conditions and also for the hologram alone are listed in Table 2. In Figure 10, the Modulation Transfer Function is plotted versus Lines per Millimeter for the noise free reconstruction and for each of the four noise conditions. This graph shows that a single line can be drawn through the points which represent the noise-free MTF's and those obtained when plates 1 and 2 were interposed. With plate 3 interposed, the MTF's are lower, but not by an appreciable amount. Only when plate 4 was interposed did the resolution drop considerably; but this was not due to signal/noise ratio, as this ratio was comparable with that from plate 1. This loss of resolution must be due to a decrease in the effective aperture of the imaging system, resulting from the very dark noise plate masking a large area of the hologram.

Figure 11 illustrates the manner in which the MTF's decrease as the signal/noise ratio decreases. For convenience, the inverse of the signal/noise ratio is plotted along the horizontal axis. In this figure, some of the discrepancies noted in the data are apparent. These discrepancies are primarily due to the difficulty of obtaining an image that is in precise focus. The MTF values from plate 4 are not included in this figure.

A sample calculation of the hologram signal/noise is included:

Light transmission of hologram = Transmitted light/Incident light = 0.38

Light transmission of plate 1 = Transmitted light/Incident light = 0.80

Intensity normalization factor for hologram = 0.38/0.80 = 2.1

Intensity normalization factor for plate 1 = 0.80/0.80 = 1

Intensity of light in Fourier plane corresponding to 240 lines/mm in hologram = Signal intensity = 275 mv

Normalized signal intensity = signal intensity normalization factor = 275 X 2.1 = 580

Intensity of light in Fourier plane corresponding to 240 lines/mm in plate 1 = Noise intensity = 1.1 mv

Normalized noise intensity = 1.1 X 1 = 1.1

Normalized signal amplitude = $\sqrt{\text{normalized signal intensity}} = \sqrt{580} = 24$

Normalized noise amplitude = $\sqrt{\text{normalized noise intensity}} = \sqrt{1.1} = 1.05$

Horizontal signal/noise = Signal amplitude/Noise amplitude = 24/1.05 = 23

Total noise amplitude = noise amplitude X 360 degrees = 380

Total signal amplitude = signal amplitude X 19 degrees = 460

Total signal/noise = Total signal/total noise = 460/380 = 1.2.

Conclusions:

It may be seen from the data that little, if any, image degradation is observed as long as the horizontal signal/noise is 10 or greater. For the case of randomly oriented noise, total signal/noise ratios of less than 0.5 show no image degradation. In fact, total ratios of 0.25 or less may give acceptable reconstructions. This is possible, of course, because the hologram itself spatially separates a large portion of the total noise from the signal.

It is of interest to note that the only poor reconstruction resulted when plate 4 was interposed. Yet plate 4 should give a signal/noise ratio comparable with plate 1. It is believed that plate 4 was sufficiently opaque as to completely mask major portions of the hologram, thus reducing the effective aperture of the system. It would seem from the data presented here that low signal/noise ratios are not prohibitive to the reconstruction of acceptable images.

The quantitative results obtained confirm the qualitative obervations made during the early phases of this work, that is, the noise plates have to be extremely bad before the image is noticeably degraded.

Future Work:

The simulation of hologram analog transmission noise has been completed.

III. MEASUREMENT OF FILM GRAIN SIZE AND ITS CONTRIBUTION TO NOISE IN WAVEFRONT RECONSTRUCTION

D. L. Wankum

Introduction:

Image formation has been achieved in a variety of forms since 1900. The early cameras recorded images on a specially prepared film which underwent a chemical change when illuminated by light. After treating the film with a developer and fixing agent, the latent image appeared. Those areas of the film which were exposed became dark in the latent image.

As time passed, better films were made and the quality of the image improved. Theories of graininess and granularity were developed by Selwyn and his followers (5, 6) to explain a long standing problem in resolution. Noise from some source in the film was degenerating the quality of an image under photographic enlargement. Large film grains were soon found to be the major source of noise. Recently this noise contribution has been more appropriately termed film grain noise.

Film grain noise became significant where holograms of weakly illuminated objects were to be recorded. When the variations in transmission of the hologram due to the weak object were of the same order as the random variations in transmittance due to film grains, the reconstructed image resolution began to decrease. The loss is noted more in large grain films such as Kodak High Contrast Copy, Tri-X, Panatomic-X, etc.

An effort is being made to study the properties of this source of noise separate from any recorded information. This is accomplished by fogging film

through exposure to incoherent light and recording the Fraunhofer diffraction pattern of the developed film. Incoherent light from a tungsten source is used instead of a coherent radiation laser source. In this way, speckling, another noise source, is prevented.

Fogging the film uniformly results in tiny deposits of silver randomly distributed throughout the emulsion after development. One can easily see these deposits under microscopic examination. These deposits are formed when the film is developed. The developer reduces exposed silver halide crystals to metallic silver, which precipitates and grows into a silver crystal. Even unexposed silver halide grains can be reduced by the developer if sufficient time is allowed; and if the film is left in the developer indefinitely, all of the silver halide is reduced to silver. Therefore, the grain size varies with the development time.

One can be certain that the grain size distribution of the particles plays a significant role in the diffraction process. For the present we can say that if the grain size distributions of two films are different, so are their diffraction patterns potentially different.

A precise definition of any diffraction pattern depends on the precision by which one can describe the diffracting medium. For films, one must describe the amplitude transmittance function of the emulsion. This is a relatively simple matter for low spatial frequencies. Let the spatial frequency increase and the situation becomes a statistical description using small opaque grains of silver having both size and density distribution properties.

In practice, one cannot measure the exact phase and amplitude of each

ray leaving the film because of the complexity and randomness of grain structure. Any information to be obtained about the film must come from its diffracted frequency power distribution spectrum, which is described by the intensity distribution of the scattered light as a function of the angular deflection from the axis of a parallel monochromatic reference beam.

Goodman (7), Helstrom (8), and Kozma (9) have all shown that random variations of film transmittance generate the "film grain noise" which is a fundamental limitation of image quality. To date no one has established the relationship for the different photographic variables such as exposure, intensity of the illuminating light, developer, development time and temperature of development affect this noise.

The diffraction pattern of an object may be observed by illuminating the object from behind by a parallel beam of coherent light. A lens (see Figure 12) is used to focus all parallel light rays of a given direction to a point in the back focal plane. The resultant amplitude at any point in the plane is the vector sum of the amplitudes of all the parallel rays coming to focus at that point.

Jenkins and White (10) show that the pattern of a diffracting screen is identical to that of its complementary screen. Complementary screens are those in which opaque spaces in one screen are replaced by transparent spaces in the other. An opaque strip and a slit of the same width, for example, have the same diffraction pattern. This principle, known as Babinet's Principle, has the advantage of enabling one to calculate the diffraction pattern of complex arrangements from the diffraction pattern of its complement.

Jenkins and White (10) also show that if the amplitude distribution of the pattern of a diffracting screen is positive, its complementary screen creates a

pattern which is negative in amplitude. This difference in sign is not detected since the square of the amplitude or the intensity is the only quantity detected by the eye or photographic film.

Born and Wolf (11) say that when a screen possesses a large number of apertures having uniform size and distributed randomly, the resulting diffraction pattern would have the same form as that from one aperture. The same is also true of its complementary screen since the diffraction pattern of complimentary screens are identical.

The complement of film grains are tiny apertures having the same size and shape as the grains. A study of the diffraction pattern produced by these grains is being made using Babinet's Principle to see what information can be obtained regarding the size and density of these grains. For purposes of holography, much emphasis is placed on predicting the intensity of the diffracted light from the emulsion. A study of the diffraction pattern should permit information, to be obtained concerning the effect of the different photographic variables present in film exposure and development. In this way, a knowledge of the physical structure of the film, the distribution of light in its diffraction pattern, and the experimental relationship between these will be established. Figure 12 shows how one can observe the diffraction of an aperture in the focal plane of a lens. Using a sufficiently large lens, the equation predicting the size of the aperture, d, is given by

$$d = \frac{k\lambda}{\sin \theta}$$

where

$$\theta = \tan^{-1} \frac{D}{f},$$

and k = 1 for a rectangular slit, 1.22 for a circular aperture; D is the distance

from the principle maximum to the first minimum; f is the focal length of the lens; and λ is the wavelength of light in the medium containing the aperture. Unlike the circular aperture, the diffraction pattern of the rectangular slit is symmetrical only along a given line perpendicular to the principal axis of the lens and lying in the focal plane of the lens. Rotate the line to some new angle and the intensity distribution along that line will be different.

The diffraction pattern of an array of many square apertures of uniform size but having no specified position or orientation on a screen resemble the diffraction pattern of a circular aperture. Well defined maxima and minima can easily be seen. The problem becomes complicated when a distribution of circular apertures of two sizes are present such that the first minima produced by one aperture falls on the second maxima produced by the other aperture. A smearing effect is produced in the diffraction pattern thus produced. An oberver unaware of the size, shape or number of apertures in the screen would be unable to predict these quantities.

Characterization by stating exact size, shape and number is not feasible in the general case. The random nature of the diffracting medium makes quantitative characterization by an oberver a statistical consideration.

Work Performed

A technique presently being investigated and developed should permit the rapid determination of the intensity distribution of light in the diffraction pattern of a fogged emulsion. This measurement is performed using a calibrated photomultiplier to determine the intensity of scattered light as a function of angle for the axis of the incident light. The basic optical system, a rotating optical spectrum analyzer, is shown in Figure 13. Rays of light

which are parallel to each other, regardless of their angular orientation θ, will be focused to a point in the focal plane of the lens. A pinhole is positioned in the focal plane to stop all rays other than those in the angular range of $\theta - \frac{\Delta\theta}{2}$ to $\theta + \frac{\Delta\theta}{2}$. The pinhole has been placed along the principle axis of the lens. The photomultiplier is centered so that light passing through the pinhole falls on the photocathode surface. Additional shielding has been used to keep stray light from striking the tube. The lens, filtering aperture (pinhole) and photomultiplier are mounted on a rotating optical bench. The object or film to be studied is positioned at the center of rotation of the rotating optical bench. This design permits measurements of large angles of diffraction. The instrument has been used extensively for studying forward scattering, but with slight modification the back-scattered spectrum can also be recorded with equal angular resolution. A total angular diffraction measurement scan of nearly 360° is practical. The angular resolution of the instrument is directly related to the pinhole diameter. For studies to date, an angular resolution of 1/2 degree was sufficient.

The rotating optical spectrum analyzer described here overcomes several difficulties inherent in most analyzers used in other laboratories for similar studies. These optical spectrum analyzers usually consist of a lens and photomultiplier positioned along the axis of the illuminating beam. The spectrum of spatial frequencies present in the object is obtained by scanning an aperture along an axis which is in the focal plane of the lens. Difficulties may arise from curvature of field of the lens as well as aberations arising from off-axis imaging.

The electron current at the output of the photomultiplier is proportional to the power of the incident light falling on the photocathode of the tube. The power of the incident light passing through the pinhole is related to its intensity by

$$I_{\Delta} = \frac{P\Delta}{A}$$

where A is the cross-sectional area of the pinhole.

Suppose that a grating on the film was a source of noise to be studied. Several bright points appear in the diffraction pattern at a distance L from the axis of the incident beam. This distance is proportional to the reciprocal lattice spacing of the grating for small scattering angles less than 10°. In general, for all scattering angles, the reciprocal lattice spacing or the spatial frequency of the grating is given by d* in the equation

$$d^* = \frac{\sin \theta}{\lambda}$$

where θ is the angle through which the radiation is scattered from the axis of the incident light. When the same grating was rotated in the plane of the film, the bright points in the diffraction pattern are rotated by the same magnitude in space. If a large number of apertures were present in a random distribution on a film and possessed the same spatial frequency, the scattered light would appear in a ring of equal brightness in the diffraction plane. The radius of this ring of brightness is L. The intensity of the light at a given point is proportional to the number of apertures having the same spatial orientation in the diffraction plane.

Normally, information concerning the total number of apertures of a given spatial frequency is more useful. The total radiation power scattered by the emulsion between θ and $\theta + \Delta\theta$ would be a measure of the total number of apertures

in the diffraction plane possessing that given spatial frequency. If the apertures are replaced by film grains, the same argument prevails. The total radiation power in an angular diffraction range between θ and $\theta + \Delta\theta$ is a quantitative measure of the grain population possessing a given spatial frequency.

The total power of light passing through an annulus of radius L and angular width $\Delta\theta$ is given by (see Figure 18)

$$P(\theta) = \int_{\theta - \frac{\Delta\theta}{2}}^{\theta + \frac{\Delta\theta}{2}} dP$$

From the geometry shown in Figure 18, $P(\theta)$ is given by

$$P(\theta) = \int_{\theta - \frac{\Delta\theta}{2}}^{\theta + \frac{\Delta\theta}{2}} I(\theta) dA$$

$$= \int_{\theta - \frac{\Delta\theta}{2}}^{\theta + \frac{\Delta\theta}{2}} I(\theta) \ 2\pi f \sin\theta \ (f d\theta) \ .$$

Since $I(\theta)$ is constant over an angular range of $\Delta\theta$, $P(\theta)$ becomes

$$P(\theta) = 2\pi f^2 \ I(\theta) \int_{\theta - \frac{\Delta\theta}{2}}^{\theta + \frac{\Delta\theta}{2}} \sin\theta \ d\theta$$

or, after integrating, utilizing trigonometric identities, and combining terms,

$$P(\theta) = 4\pi f^2 \sin\frac{\Delta\theta}{2} \ I(\theta) \sin\theta \ .$$

Define $F(\theta) = \frac{P(\theta)}{P_t}$ where P_t is the total radiant energy scattered forward

through the emulsion. Then

$$F(\theta) = \frac{4\pi f^2 \sin \frac{\Delta\theta}{2}}{P_t} I(\theta) \sin \theta \ .$$

If the radiant power-to-voltage conversion factor for the photomultiplier is given K in watts per volt, $F(\theta)$ can be written in terms of the photomultiplier output as

$$F(\theta) = \left[\frac{4\pi K f^2}{A} \sin \frac{\Delta\theta}{2} \right] \frac{\sin \theta}{P_t} V$$

where A is the area of the pinhole in meters^2, shown in Figure 13, and V is the potential developed in volts at the output of the photomultiplier.

Figures 14, 15, 16 are semi-log plots of the normalized power distribution function $F(\theta)$ for three different films exposed and developed using standard developers and development times. These films are Kodak Plus-X, High Contrast Copy, and Panatomic-X respectively. Figure 17 presents a comparison of the scattering angles versus $F(\theta)$ for the three types of films when exposed to approximately the same optical density. Tables 3, 4, and 5 present the development information on each film. In Figures 14, 15, and 16 it may be seen that low spatial frequencies tend to predominate in the grain distribution.

Figure 14 shows $F(\theta)$ for Plus-X Pan exposed to different densities. Note the broad maximum of curve 4 in $F(\theta)$ around 20° for a density of 0.85. This minimum indicates a preponderance of grains whose average diffraction pattern shows a maximum around 20°. By Babinet's Principle, since film grains are opaque and represent stops rather than apertures, this maximum corresponds to a mean grain diameter of ~2.3 microns assuming a circular aperture. However, from the small amplitude of the maximum it is clear that a large distribution

of grain sizes is present. At lower densities the peak appears to move to smaller angles indicating, on the average, an increase in grain size. This observation agrees with other known facts. Large grains are the most sensitive and so predominate at low light levels. At higher densities a broad maximum exists because of the wide range of film grain sizes which make up the diffracting object.

These results may be compared with Panatomic X (see Figure 16) for which, at density = 0.8, the maximum occurs at 25° (curve 4). The most frequently occurring grain sizes are somewhat smaller (1.8 microns) than those associated with Plus-X Pan when exposed under similar conditions. Note again the breadth of the maximum. All wide latitude films are characterized by a large range of film grain sizes.

The High Contrast Copy film grain size distribution is in contrast to the above results. For optical densities as low as 0.43, where only the larger grains are exposed, the maximum occurs at 30°, indicating that 1.5μ micron sized grains predominate. At a density of 1.52 the mean grain size remains unchanged. High Contrast Copy film, as are all high resolution films, is characterized by uniform grain sizes. The mean grain size of Panatomic-X and Plus-X Pan are not appreciably larger than that of High Contrast Copy film; however, there is a substantial population of large grains which are essential for exposure latitude (a good gray scale) but detrimental to resolution.

Film grain noise characterization in the manner outlined in this report will be continued in a systematic manner. An attempt will be made to find

out how the photographic variables such as exposure time, intensity of light used to expose the film, developer, development temperature, development time, and density of the film affect film grain noise. Secondary diffraction processes, if any, will be considered relative to their effect on the quantitative evaluation of this technique.

IV. THE WASH-OFF RELIEF PROCESS FOR IMAGE STORAGE

G. K. Wallace

Introduction:

Using normal processing procedures, photographic emulsions act as nonlinear light intensity detectors in that they store information as differences in optical density. These differences in density may be stored linearly with changes in intensity over a limited range. In addition to variations in optical density, variations in the thickness of the photographically processed emulsion (developed, stopped, fixed) also result. This variation, or relief, is especially evident in Kodak 649-F plates and occurs because more undeveloped silver halide is removed during fixing from those areas of the emulsion which have been only briefly exposed to light than from the more heavily exposed portions of the emulsion.

If the photographic image were to be bleached, the variation in optical density is removed, but the relief of the gelatin image is increased. The bleaching process leads to the formation of a colorless compound which is insoluble in water in those areas where a silver image existed. This fact has been utilized in the formation of phase holograms. These holograms rely upon the relief of the bleached emulsion rather than variations in optical density to form reconstructed images. The images so formed are known to exhibit more brightness than those obtained from normally processed holograms.

Further increase in relief can be caused in the emulsion if the wash-off relief process is applied to the bleached photographic plates (see Appendix 1).

The actual wash-off technique is a hot water treatment preceded by a series of steps that allows selective removal of gelatin from areas of lower optical density in the original image. When the emulsion is unexposed, it is possible to completely remove the emulsion. With increasing optical density, less and less emulsion is removed by wash-off.

It has been demonstrated by Dodd (12) that wash-off relief holograms can produce images which may be brighter than those obtained from bleached holograms. The purpose of this investigation was to become familiar with the process so that it can be better understood and possibly utilized as a method of storing optical information possessing additional desirable properties.

Work Performed:

It is well known that holograms which have been bleached reconstruct images of greater intensity than similar holograms which have not undergone the bleaching process. It was desired to see whether the intensity of the reconstructed images from bleached holograms varied with the exposure time of the hologram and with the spatial frequency recorded in the emulsion. As a preliminary step, a series of grating patterns was made on Kodak High Contrast Copy Film by recording the interference pattern which results when two beams of parallel, coherent light intersect at an angle. The patterns resulting from varying interference angles were recorded at several different exposure times on a single roll of film. The film was developed using the manufacturer's recommended procedure, stopped with a one-minute wash in running water, and fixed with a non-hardening fixer. Each of the photographically recorded interference gratings was placed in turn in the beam of a 1 milliwatt Helium Neon laser and the number of diffraction orders detectable by the naked eye

was observed. The gratings then received the bleaching treatment, after which they were replaced in the 1 milliwatt laser beam and the number of diffraction orders visible were again observed. The observations are tabulated in Tables 6 and 7. Table 6 shows that the number of observed higher orders from each grating increases after the grating has been bleached. In Table 7, the number of higher orders observed at a given grating spatial frequency is compared for various exposure times. The number of higher orders observed was found to depend upon the spatial frequency and also upon the exposure time. It appears that there may be an optimum exposure time for the production of a maximum number of higher orders at a given spatial grating.

An interesting observation was made during the study of these interference gratings. For the 25 lines/mm gratings, which were exposed for times of 1/150, 1/100, and 1/50 seconds, the intensity of the ±1, ±2, and ±3 diffraction orders appeared to be equal to or greater than that of the zero order. The reason for the relatively high intensity of these higher orders has not as yet been determined.

The steps in the wash-off relief process consist of developing, bleaching, and the actual wash-off of portions of the emulsion. This sequence of steps makes it possible to record information in the emulsion and then study and compare individually the separate effects of development, bleaching, and wash-off on each individual emulsion. It was decided to record photographically a series of interference gratings similar to those used in the preliminary work. The magnitude of the emulsion relief could be measured after each of the steps - development, bleaching, and wash-off - and also the brightness of the various diffraction orders present after each step could be compared

in a quantitative manner. A reflection-type microscope interferometer was to be used to measure the relief variations in the emulsions. In this device, the surface of the emulsion constitutes one of the reflecting surfaces of the interferometer. The second reflecting surface of the interferometer is a mirror which can be adjusted so that various finite fringe presentations can be observed. An example of the type information obtainable from this instrument is illustrated in Figure 20, which is the interferogram of an emulsion which has recorded an interference grating similar to those described previously. The finite fringe interferogram indicates a difference in height between "peaks" and "valleys" in the emulsion of approximately 6½ wavelengths of light. Since the interferogram was obtained by reflecting light from the surface of the emulsion, the actual magnitude of the emulsion relief is only 3¼ wavelengths. This interferogram was obtained using a sodium lamp as a source of illumination, so the magnitude of the relief of the emulsion is 3¼ times 0.59 micron, or 1.9 micron relief.

The interferometer to be used in the experiments became inoperative shortly before the series of interference gratings were ready for evaluation. As a consequence, none of the quantitative data has been obtained as yet. The evaluation of the effect of the wash-off relief process upon the brightness of the higher diffraction orders obtained from simple interference gratings remains as "work to be done".

While the microscope interferometer was still operable, several observations were made concerning emulsion relief which may give an indication of the magnitude of the relief which may be encountered. A Kodak 649-F photographic plate was used to record a simple interference grating. After it

had been developed, fixed, and dried in ambient air for a few hours, the difference in relief between the lighter and more heavily exposed portions of the grating was found to be approximately 0.3 micron. Several days later, after the emulsion had lost all of its excess moisture, the relief difference decreased to approximately 0.1 micron. The emulsion was then bleached, after which the magnitude of the emulsion relief became 1.9 micron. The interferometric determination of the relief of this bleached grating is shown in Figure 20. Similar observations made on Kodak High Contrast Copy Film showed no detectable relief after normal development. Bleaching the emulsion resulted in only about 0.3 micron relief, while the wash-off step added an additional 0.5 micron of relief.

When the microscope interferometer became inoperable, an attempt was made to measure the magnitude of the emulsion relief holographically. A typical double exposure holographic interferogram was made as shown in Figure 19. The object was a frame of Kodak High Contrast Copy Film on which an interference grating has been recorded photographically. The spacing between interference lines in the object grating was such that three line pairs were recorded in the frame of the emulsion. The film had been developed normally and then bleached. The interferogram which was obtained when the doubly exposed hologram of the object grating was reconstructed is shown in Figure 21. Irregularities in the film base are of a larger magnitude than the emulsion relief, and thus mask the detail of interest. A similar double exposure hologram was recorded using the same object, except that the film frame had now undergone the wash-off relief step. The reconstruction from this holographic interferogram is shown in Figure 22. There is some apparent difference between the fringes of

Figures 21 and 22, but again the irregularities in the film base do not allow us to observe directly the emulsion variations. A differential interferogram was obtained which showed only the effect of the emulsion that had been removed by the wash-off process. This interferogram was obtained in the following manner. The hologram which had been made of the emulsion after bleaching only was replaced in the position where it had been made. The film, after the wash-off step, was placed in the position it occupied when the holograms were formed. The hologram, upon illumination by the reference beam, reconstructed the diffraction pattern of the bleached emulsion. The washed-off emulsion illuminated by the original object beam and its diffraction pattern were coincident with the hologram reconstruction. In the resulting interferogram, the irregularities of the film base were cancelled out, and the finite fringe pattern observed was due only to changes in the object which occurred between the bleaching and the wash-off steps.

A finite fringe differential interferogram of the same object illustrated in Figures 21 and 22 is shown in Figure 23. In this example, the variation in the fringes appear to show that light traveling through the higher portions of the emulsion travel approximately 3/4 wavelength farther than those which pass through those portions of the emulsion which have had more gelatin washed off. This interferogram was made with 6328 Å light and was produced by transmission rather than by reflection, as in the case of the microscope interferometer. The index of refraction of the emulsion must be considered when calculating the magnitude of the height variations in the emulsion. Assuming the index of refraction of the emulsion to be approximately 1.5, the magnitude of the relief contained in the emulsion shown in Figure 23 due to

the wash-off step only would be 0.3 micron.

Holographic differential interferometry is a useful method for studying the increase of relief in the emulsion after each processing step, but one that is very time consuming if a large number of emulsions are to be studied. For this reason, it was decided to await the repair of the microscope interferometer before conducting further studies.

In the interim, some quantitative studies have been carried out utilizing Kodak 649-F photographic plates. It had been feared that the wash-off treatment might cause reticulation or "orange peel" of the emulsion because of the poor adhesion between the gelatin and the glass. No reticulation was observed, however, when the temperature of the water used in the wash-off step was slowly increased to the proper value and then again slowly cooled before removing the photographic plate from the wash. Although no measurements have been made, it has been observed that definite relief can be seen on the surface of the emulsion of 649-F plates between areas which had been exposed for different periods of time but which were so dark after development that no difference in optical density could be detected by the eye. The complete removal of unexposed portions of the emulsion has also been accomplished.

One further observation should be reported. An interference grating with a spatial frequency of 25 lines/millimeter was recorded on Kodak High Contrast Copy Film. Various exposure times were used in recording this pattern on a single strip of film. The film was developed, bleached, and washed-off. Upon examining the diffraction orders which were produced when the gratings were illuminated with the 1 mw Helium Neon laser, it was observed that one

particular grating on the film strip produced a diffraction pattern in which the first order diffracted beam was very dim, while the second and third orders appeared quite intense. When this particular grating was illuminated with white light, it could be seen that the first order diffracted beam was indeed present, but that it preferentially contained the blue and green portions of the spectrum while supressing the longer wavelengths. This phenomenon has not been explained, and as yet a duplication has not been attempted in this laboratory.

Conclusions:

The wash-off relief process shows some promise as a means of recording information in photographic emulsions. The process makes it possible to increase the magnitude of emulsion relief beyond that possible by bleaching alone, making it possible to reconstruct images from wash-off holograms on low resolution photographic films which may be brighter than those images which are obtained after bleaching alone. Several interesting phenomena have been observed during preliminary studies with bleached and wash-off gratings. These include observations in which some of the higher diffraction orders appear to be more intense than the zero order, and a single instance wherein the longer wavelengths were supressed in the first diffraction order.

Future Work:

The study of the wash-off relief process will continue with the goal of optimizing the process and controlling the degree of wash-off with some precision.

The quantitative investigation of the intensity of the diffraction orders produced by interference gratings after each of the steps of development,

bleaching, and wash-off should be carried out. This investigation should lead to some conclusions concerning the effect of emulsion relief upon the intensity of hologram reconstructions and thus permit a hologram recorded on a given photographic medium to be processed in such a way as to maximize the reconstructed image intensity.

An attempt will be made to relate emulsion relief to the intensity of certain diffraction orders obtained from gratings and to the supression of certain wavelengths in particular diffraction orders.

The investigation of different types of recording media, as well as seldom used processes and techniques which are not suitable for conventional photography but which may possess characteristics suited for optical data storage should be undertaken.

APPENDIX I

The Wash-Off Relief Process was performed as follows:

(a) Expose film normally but through the back. The more heavily exposed regions will then be nearest the film base, and proper relief development of the image is then possible.

(b) Develop exposed film using the manufacturer's recommended developer. Development times are specified in the Kodak Manual for each particular Kodak film and these times were found to be satisfactory. All steps should be performed with continuous agitation.

(c) The stop bath is a one-minute wash in running water. An acid stop bath should not be used. As in normal film processing, all steps should be performed at the same temperature.

(d) The film is fixed in a non-hardening fixer; for convenience, Kodak F-24 Fixer was used. The film is then washed in running water for about ten minutes to clear it of any soluble residual chemicals.

(e) After drying at room temperature, the emulsion is well "set-up" and one can proceed to the bleaching step. For convenience, the bleach packet of Kodak Chromium Intensifier is used. The bleach tans the gelatin dependent on the blackness in the original silver image. Terminate when the black image is completely reduced. The bichromate bleach selectively hardens the emulsion in proportion to the image optical density.

(f) The film is again placed in running water and allowed to wash for several

hours to remove the unhardened gelatin. Temperature is gradually increased (to minimize stress on the hardened areas) to 40°C to 50°C, but no higher than necessary to slowly dissolve the unhardened gelatin. Reduce temperature gradually back to room temperature.

(g) Dry the emulsion in still air at room temperature (in order to minimize damage due to peeling, cracking and shifting in the gelatin). This method may require several days before complete removal of water trapped in the gelatin is effected. This magnitude of time was found to be necessary in order to get consistent results.

REFERENCES

(1) K. Stetson and R. Powell, J. Opt. Soc. Am., 56; 1161 (1966).

(2) L. Heflinger, R. Wuerker and R. Brooks, J. Appl. Phys., 37; 642 (1966).

(3) R. Wuerker, L. Heflinger and R. Brooks, Naecon Conf., Dayton, Ohio, May 18, 1966.

(4) R. Collier, E. Doherty and K. Pennington, Appl. Phys. Lett., 7; 223 (1965).

(5) L. A. Jones and G. C. Higgins, J. Opt. Soc. Am., 35; 435 (1945).

(6) L. A. Jones and G. C. Higgins, J. Opt. Soc. Am., 36; 203 (1946).

(7) J. W. Goodman, J. Opt. Soc. Am., 57; 493 (1967).

(8) C. W. Helstrom, J. Opt. Soc. Am., 56; 433 (1966).

(9) A. Kozma, J. Opt. Soc. Am., 58; 436 (1968).

(10) Francis A. Jenkins and Harvey E. White, "Fundamentals of Optics", 3rd Ed., McGraw-Hill, New York, p. 376 (1957).

(11) Max Born and Emil Wolf, "Principles of Optics", 2nd Rev. Ed., Macmillan Company, New York, p. 400 (1964).

(12) Jack G. Dodd, University of Arkansas, Progress Report, NASA Grant NsG 713, September 12, 1967, p. 27.

TABLE 1

Signal/Noise Value for Spatial Frequency of 240 lines/mm

	Hologram	Plate 1	Plate 2	Plate 3	Plate 4
Light Transmission of Plate (%)	38	80	26	5	1
Normalization Factor for Light Transmission	2.1	1.0	3.1	16	80
Relative Intensity of Scattered or Refracted Light	275	1.1	2.1	1.36	0.021
Normalized Intensity of Scattered or Refracted Light	580	1.1	6.5	22	1.7
Normalized Amplitude of Scattered or Refracted Light ($\sqrt{I}$)	24	1.05	2.5	4.7	1.3
Horizontal Signal/Noise	-	23	9.6	5.1	18
Horizontal Noise/Signal	-	0.043	0.10	0.20	0.056
Total Signal/Noise (Horizontal Signal/Noise x $\frac{19}{360}$)	-	1.2	0.51	0.27	0.95
Total Noise/Signal	-	0.83	2.0	3.7	1.1

TABLE 2

Modulation Transfer Function for Various Image Lines With Each Noise Plate

	lines/millimeter					
Noise Plate	8	9	11	13	15	18
No Noise Plate	0.82	0.68	0.61	0.39	0.20	0.07
A	0.81	0.69	0.53	0.42	0.20	0.06
B	0.75	0.68	0.55	0.48	0.29	0.08
C	0.64	0.49	0.40	0.28	0.14	-
D	0.20	0.19	0.09	-	-	-

TABLE 3

Development Information for Kodak Plus-X Pan Film
(Developed in D-76 (1:1) for 7 minutes at 70°F)

Frame No.	Relative Exposure Time (seconds)	Transmittance	Density
1	0.1	0.37	0.37
2	0.2	0.30	0.52
4	0.8	0.14	0.85
5	1.6	0.11	0.96
10	25.0	0.040	1.40
12	100.0	0.028	1.60

TABLE 4

Development Information for Kodak High Contrast Copy Film
(Developed in D-19 for 5½ minutes at 70°F)

Frame No.	Relative Exposure Time (seconds)	Transmittance	Density
4	0.4	0.47	0.33
5	0.8	0.37	0.43
6	1.6	0.20	0.70
7	3.2	0.03	1.50

TABLE 5

Development Information for Kodak Panatomic X
(Developed in D-76 (1:1) for 8 minutes at 70°F)

Frame No.	Relative Exposure Time (seconds)	Transmittance	Density
1	0.1	0.42	0.38
2	0.2	0.37	0.43
3	0.4	0.26	0.58
4	0.8	0.16	0.80
6	3.2	0.080	1.0
8	13.0	0.047	1.3
11	100.0	0.032	1.5

TABLE 6

The Effects of Bleaching Process on the Number of Higher Side Order Images Observed from Kodak High Contrast Copy Film (35mm) Interference Gratings

SPATIAL FREQUENCY OF GRATING (lines/mm)	HIGHEST ORDER OBSERVED	
	Ordinary Developed Grating	Bleached Grating
25	±3	±9
33	2	6
55	1	4
79	1	3
80	1	3
81	1	4
93	1	3
132	1	2
186	0	2
226	0	1
383	0	1

TABLE 7

Number of Higher Diffraction Orders Observable from Bleached Interference Gratings of Various Spatial Frequencies Recorded at Several Exposure Times on Kodak High Contrast Copy Film (35 mm)

Spatial Frequency (lines/mm)	Exposure Time (seconds)											
	1/150	1/100	1/50	1/25	1/2	1	2	4	8	15	30	60
25	9*	6	5	4	2	2	2	2	1			
33	6	4	4	5	1	1	1	1	1			
79	3	3	2	2	1							
80	3	3	2	2								
81	3(2)**	4(2)	4(2)	3(1)	1(0)	1(0)	1(0)	1(0)	1(0)	1(0)	1(0)	1(0)
93	2	2	3	2								
132	2	2	2	1								
186	1	2	1	1								
226	1	1	1	1								
383	1	1	1	1								

*All images occur in pairs (±)
**Numbers in parentheses indicate the number of higher order images corresponding to a photographically processed (developed, stopped, fixed) interference grating for comparison with images from the bleached interference grating.

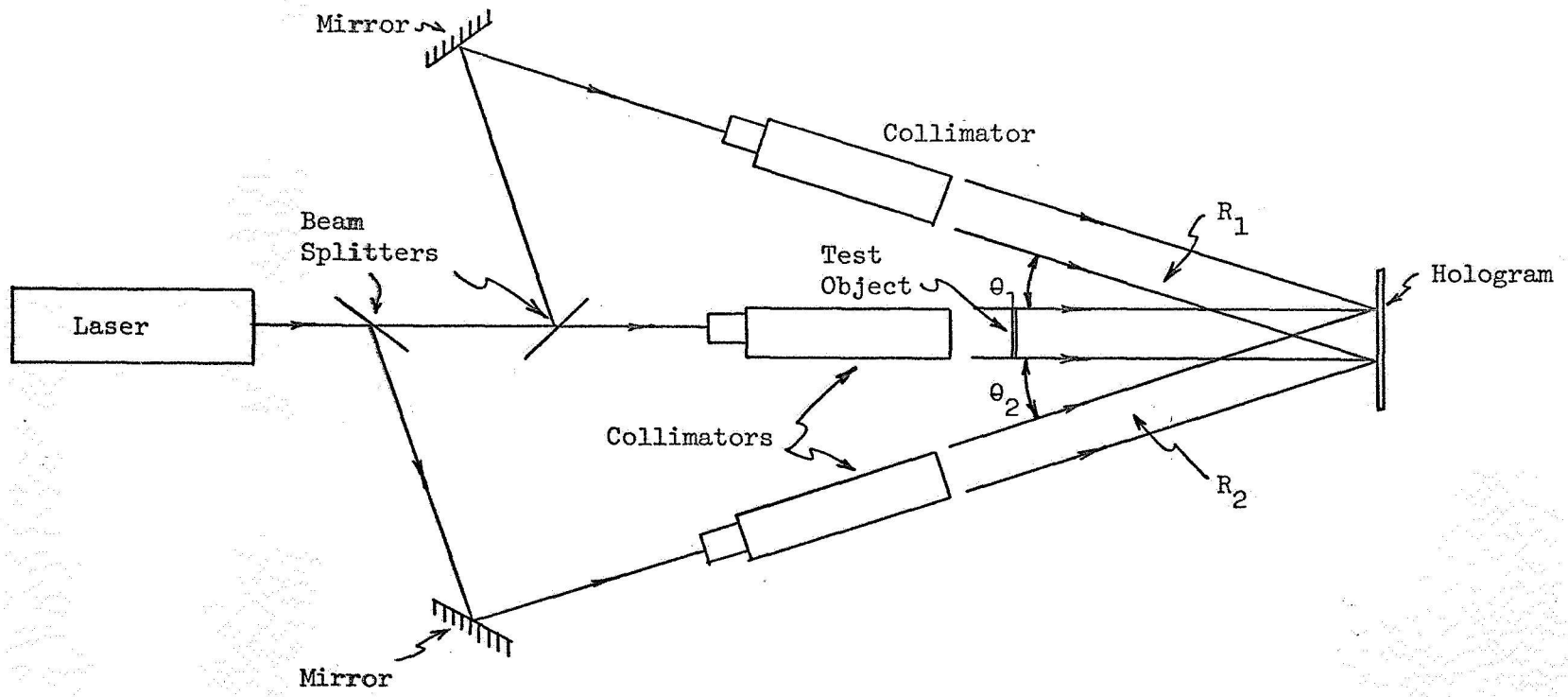

Figure 1

HOLOGRAM RECORDING ARRANGEMENT

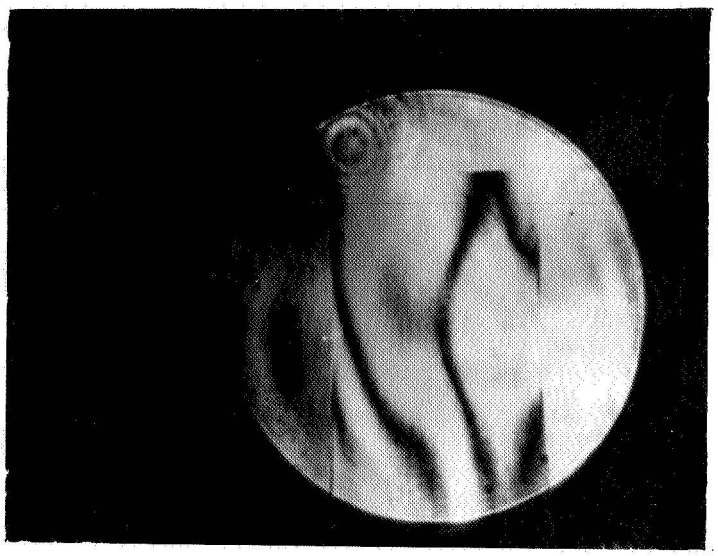

Figure 2

ZERO ORDER INTERFEROGRAM RECONSTRUCTED FROM DUAL-REFERENCE HOLOGRAM

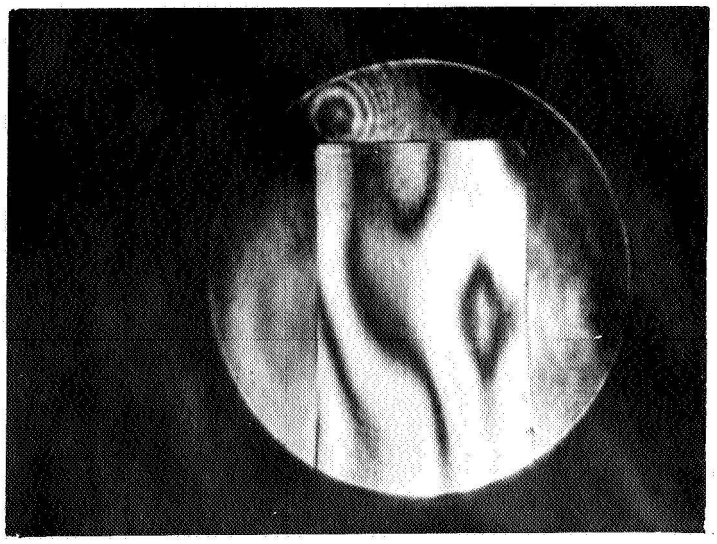

Figure 3

INTERFEROGRAM RECONSTRUCTED WITH PHASE OF COMPARISON BEAM SHIFTED 180°

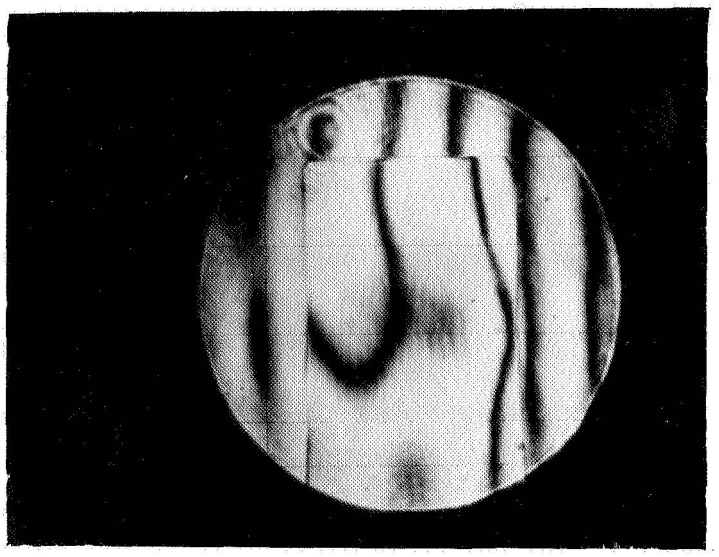

Figure 4

FINITE FRINGE INTERFEROGRAM OBSERVED WHEN θ_2 IS ALTERED

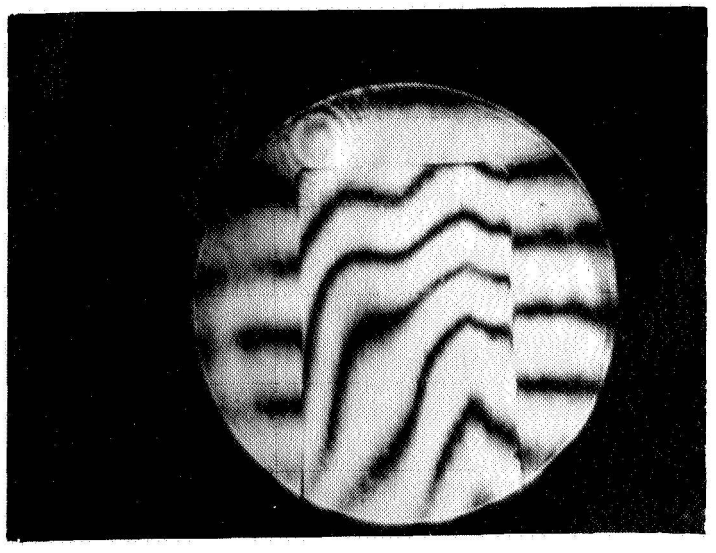

Figure 5

FINITE FRINGE INTERFEROGRAM OBSERVED WHEN A CHANGE IN THE VERTICAL ANGLE OF θ_2 IS INTRODUCED

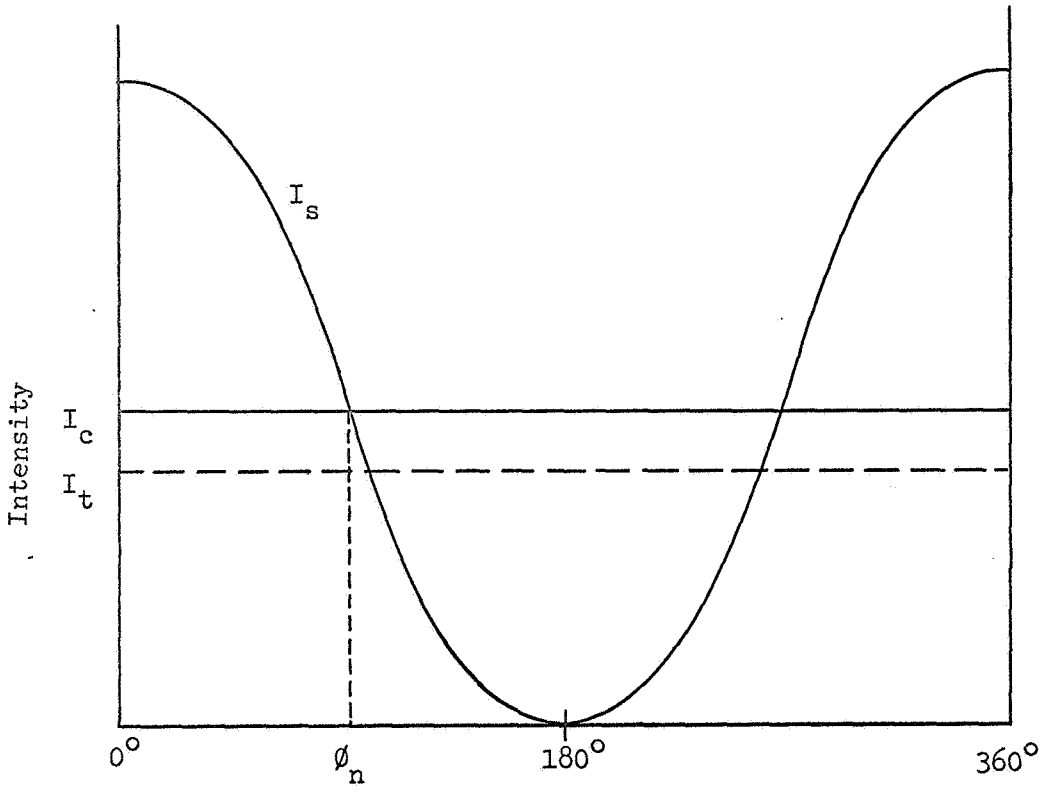

Figure 6

VARIATION OF THE INTENSITY OF TWO COHERENT BEAMS
AS THEIR RELATIVE PHASE IS ALTERED

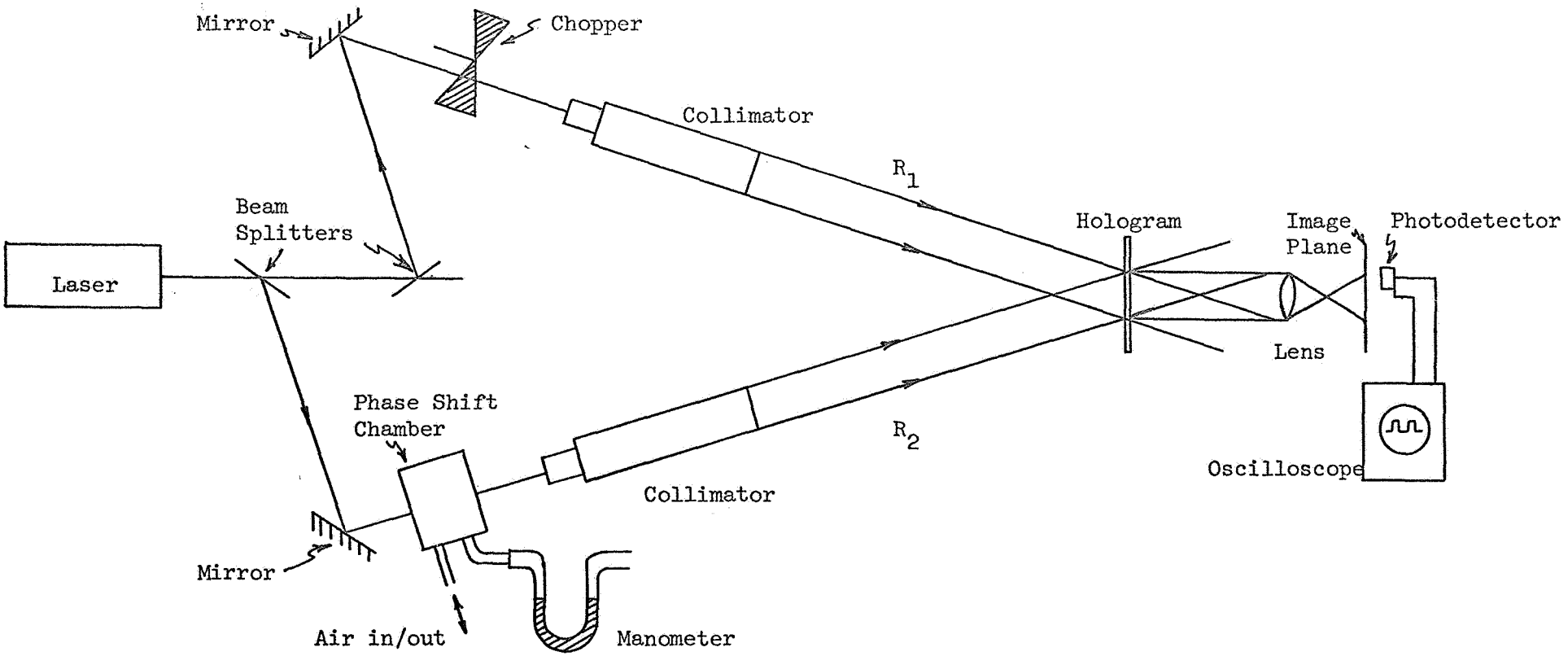

Figure 7

METHOD USED TO MEASURE SMALL PHASE DEVIATIONS IN A HOLOGRAPHICALLY RECORDED OPTICAL FIELD

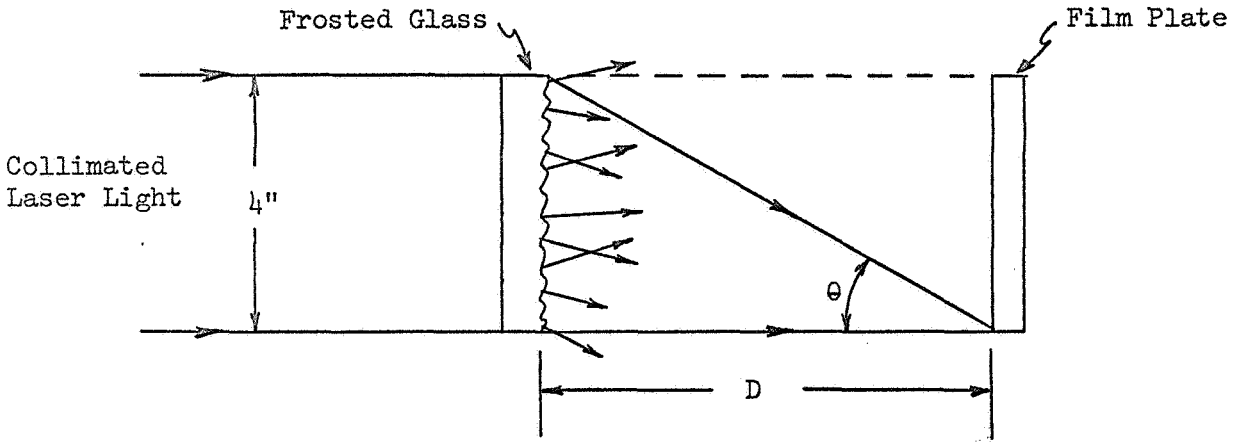

Figure 8

METHOD OF OBTAINING RANDOM NOISE PLATE

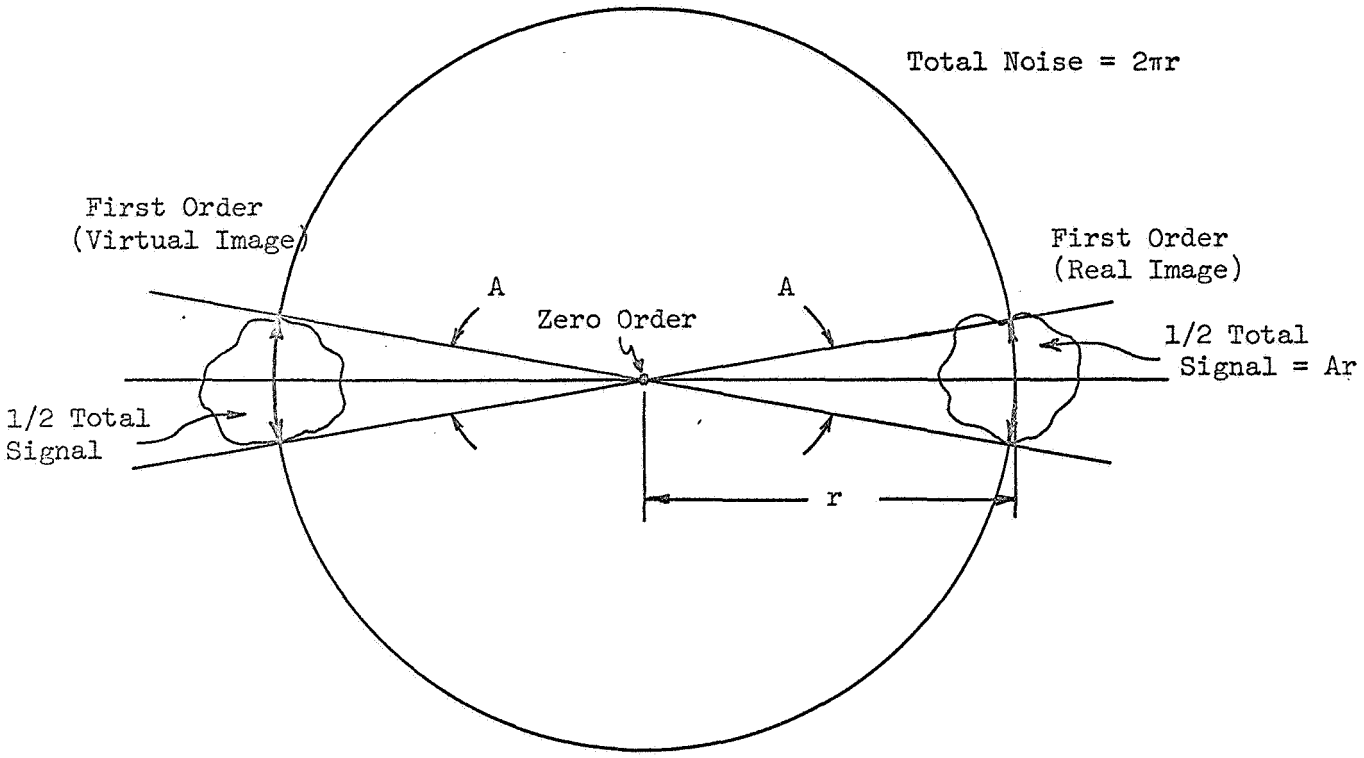

Figure 9

TOTAL SIGNAL AND NOISE FROM OPTICAL FOURIER ANALYSIS OF HOLOGRAM

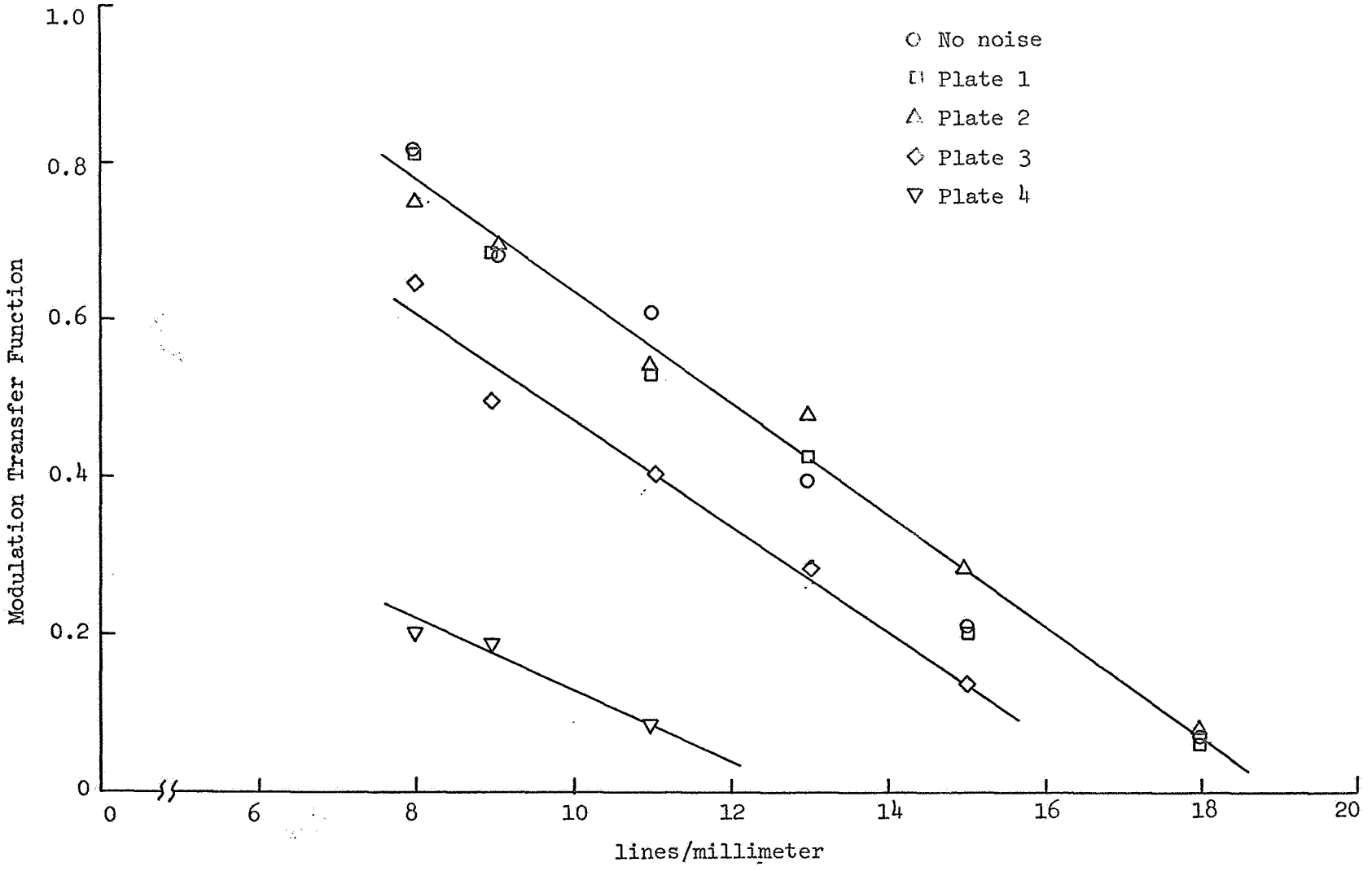

Figure 10

IMAGE M.T.F. VERSUS IMAGE lines/mm FOR HOLOGRAM AND NOISE PLATE

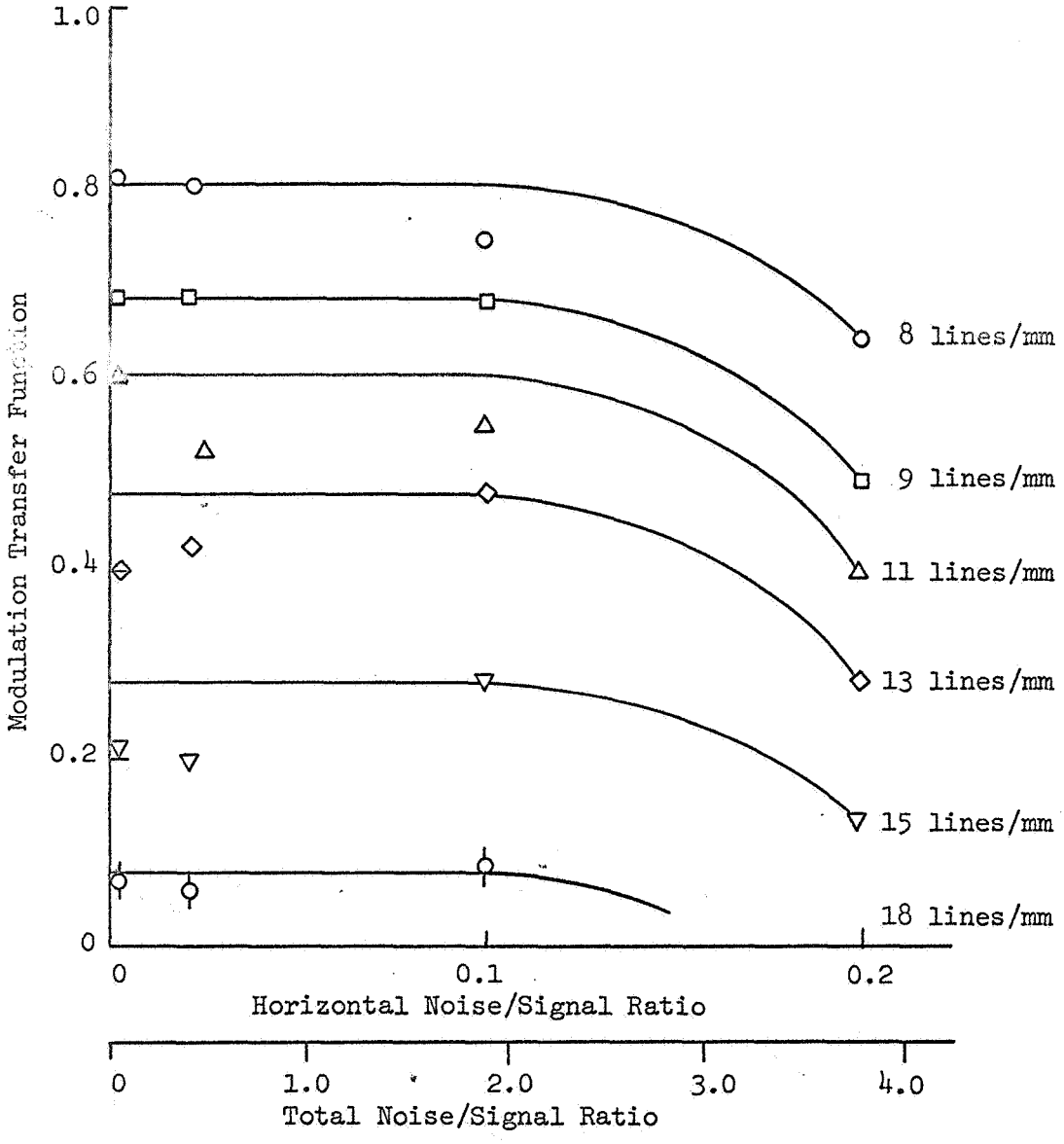

Figure 11

IMAGE M.T.F. Versus HOLOGRAM NOISE/SIGNAL RATIO

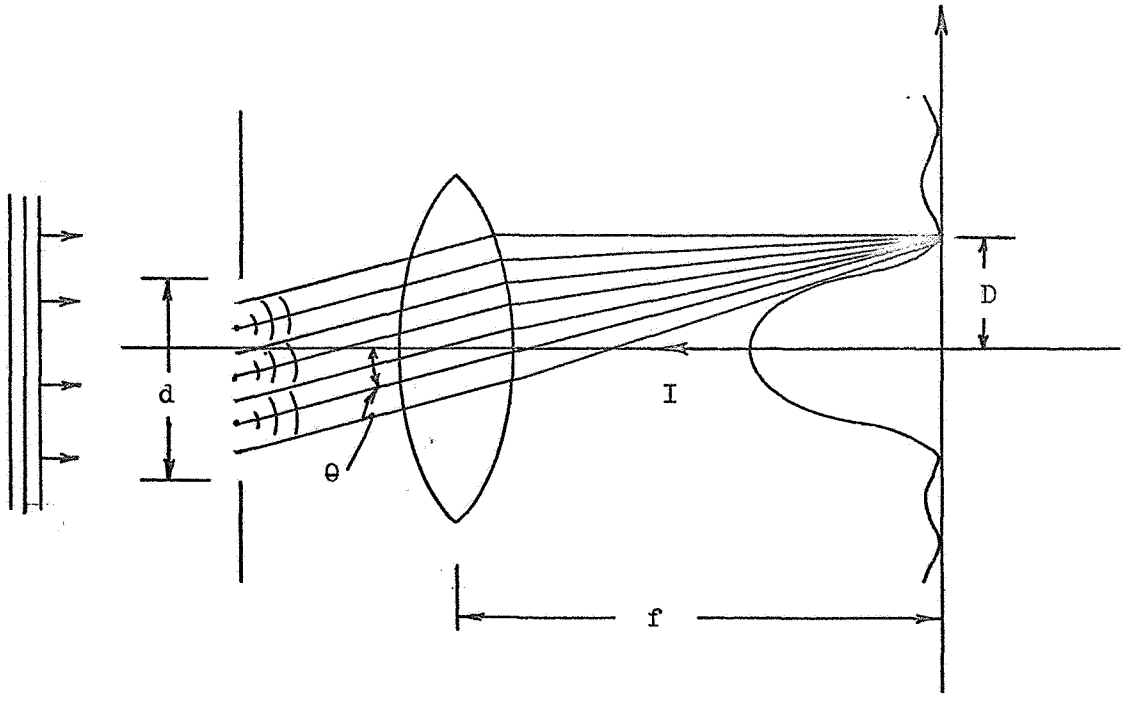

Figure 12

DIFFRACTION PATTERN OF A SINGLE SLIT OF WIDTH b

(The first minima occurs when $b = \lambda/\sin\theta$)

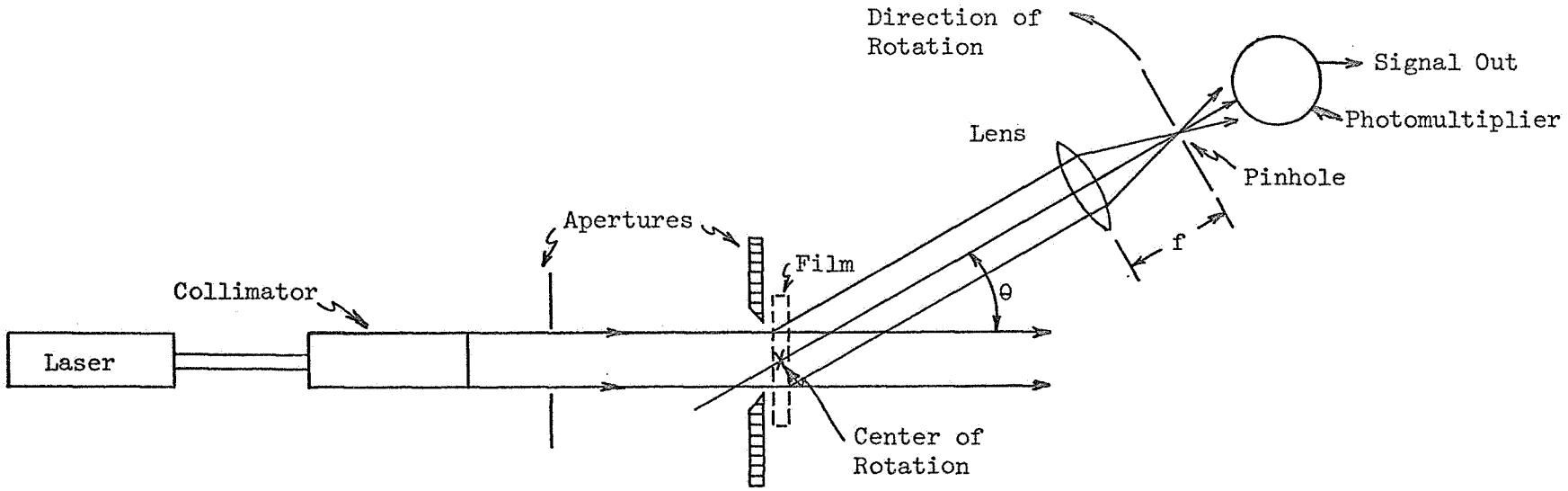

Figure 13

ROTATING OPTICAL SPECTRUM ANALYZER DEVELOPED IN THIS LABORATORY

(The lens, pinhole and photomultiplier are mounted on an optical bench having a center of rotation at the film)

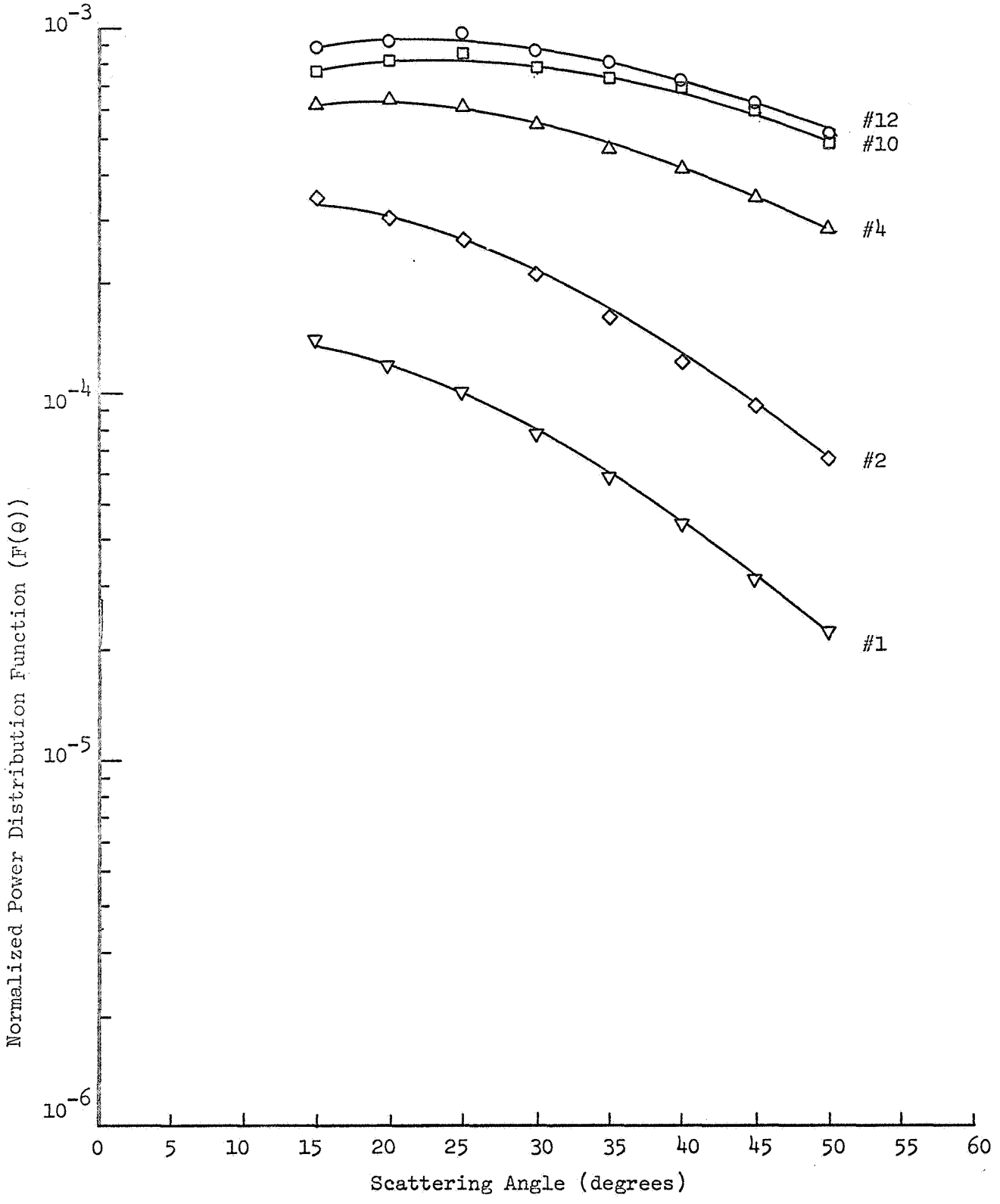

Figure 14

Normalized Power Distribution Function for Kodak Plus-X Pan Film Plotted Against the Angle the Light Is Scattered Away from the Axis of the Incident Light

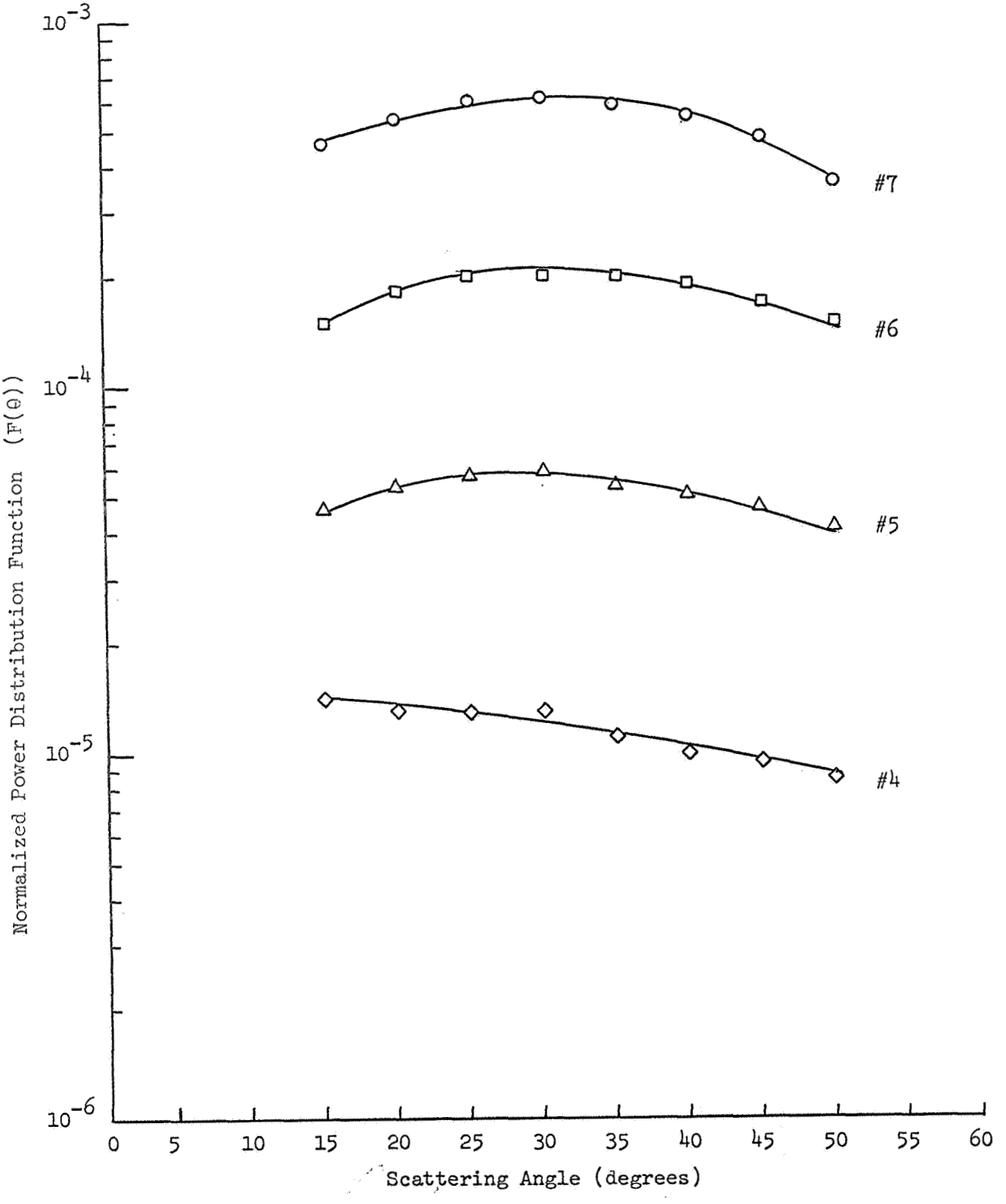

Figure 15

Normalized Power Distribution Function for High Contrast Copy Film Plotted Against the Angle the Light Is Scattered Away from the Axis of the Incident Light

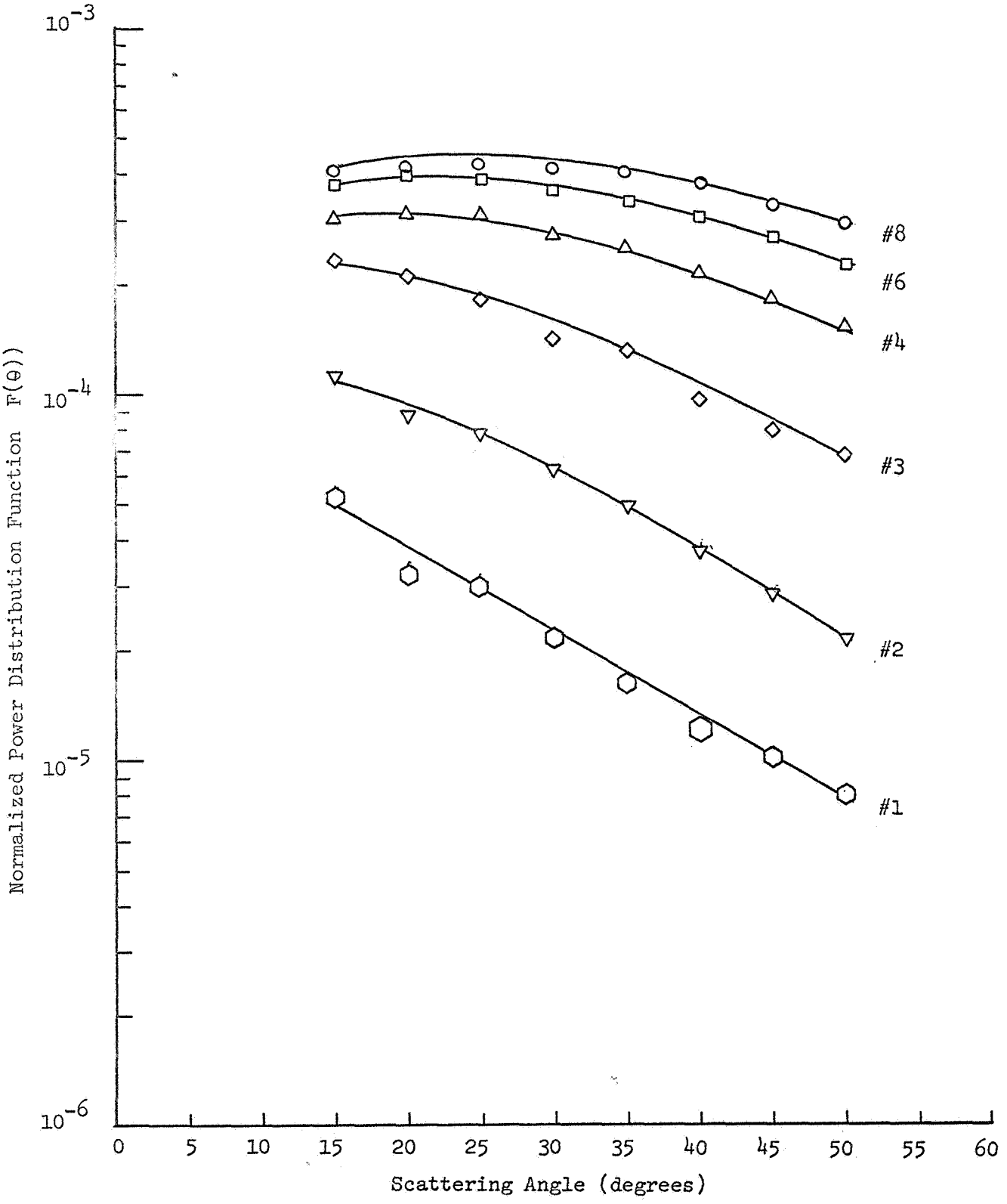

Figure 16

Normalized Power Distribution Function for Panatomic X Film Plotted Against the Angle the Light is Scattered Away From the Axis of the Incident Light

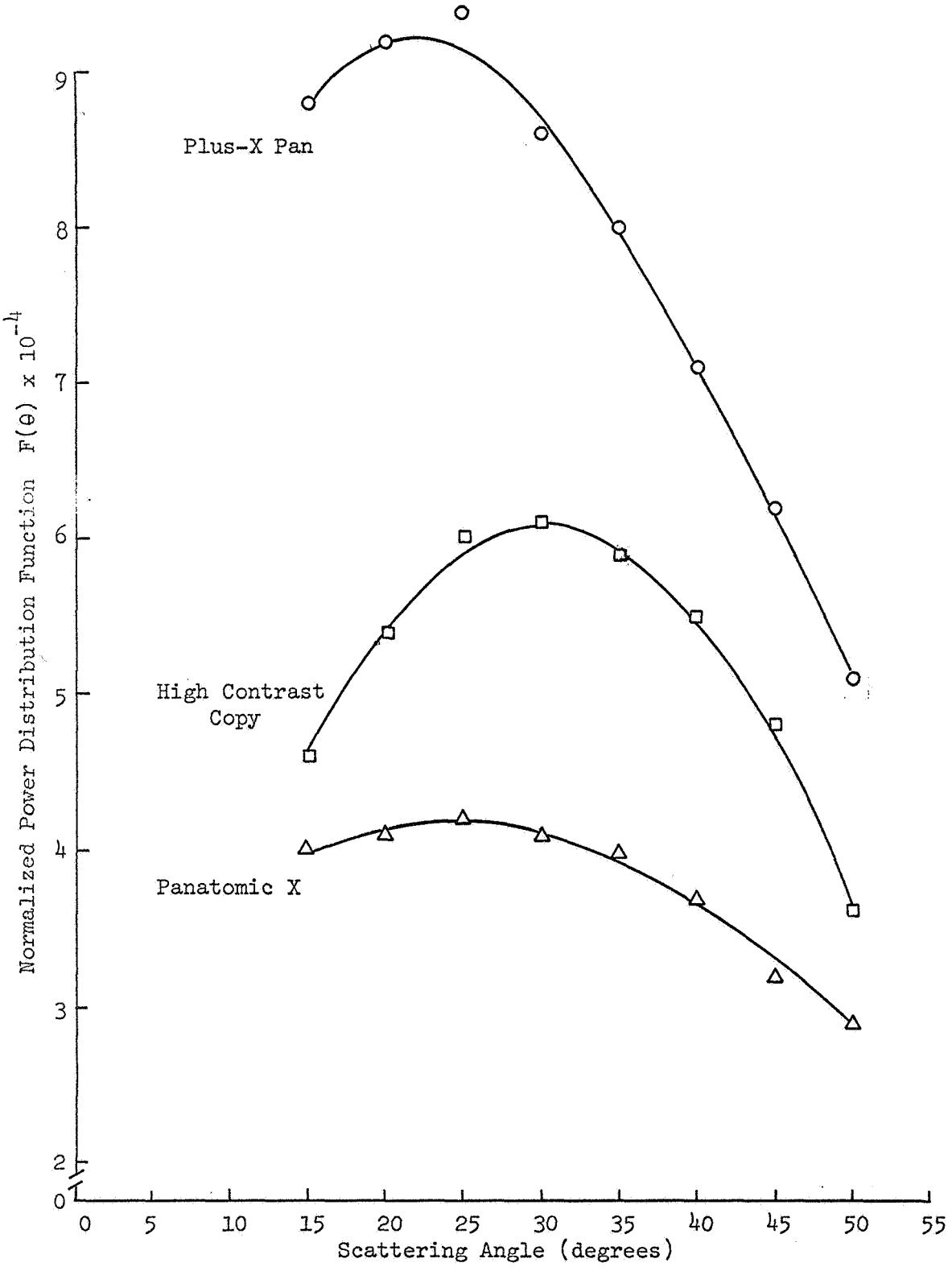

Figure 17

Normalized Power Distribution Function for the Types of Film Exposed to Approximately the Same Optical Density

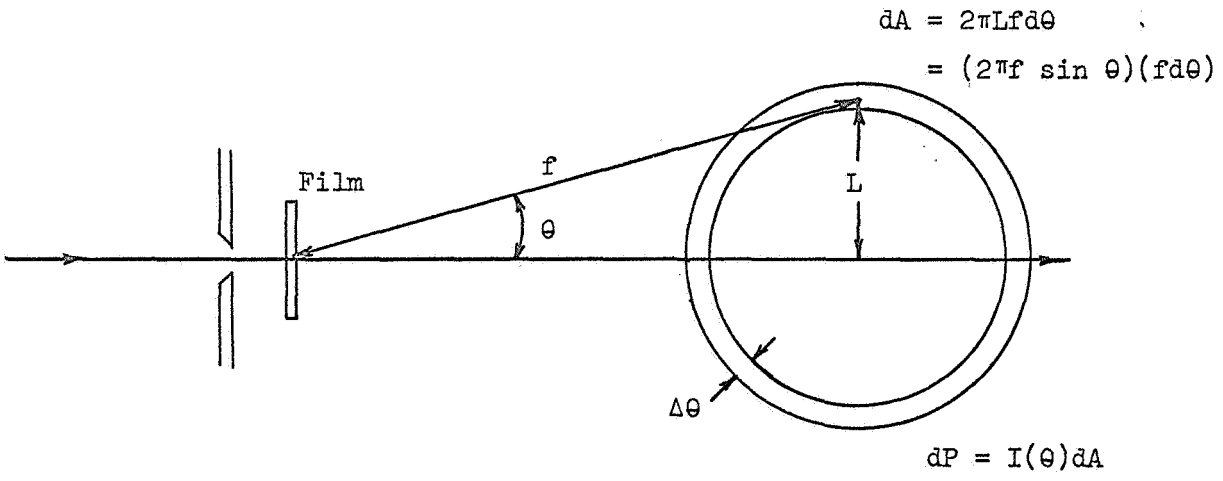

Figure 18

SCATTERING GEOMETRY USED TO NORMALIZE THE TOTAL RADIANT POWER PASSING THROUGH AN ANNULUS OF ANGULAR WIDTH $\Delta\theta$

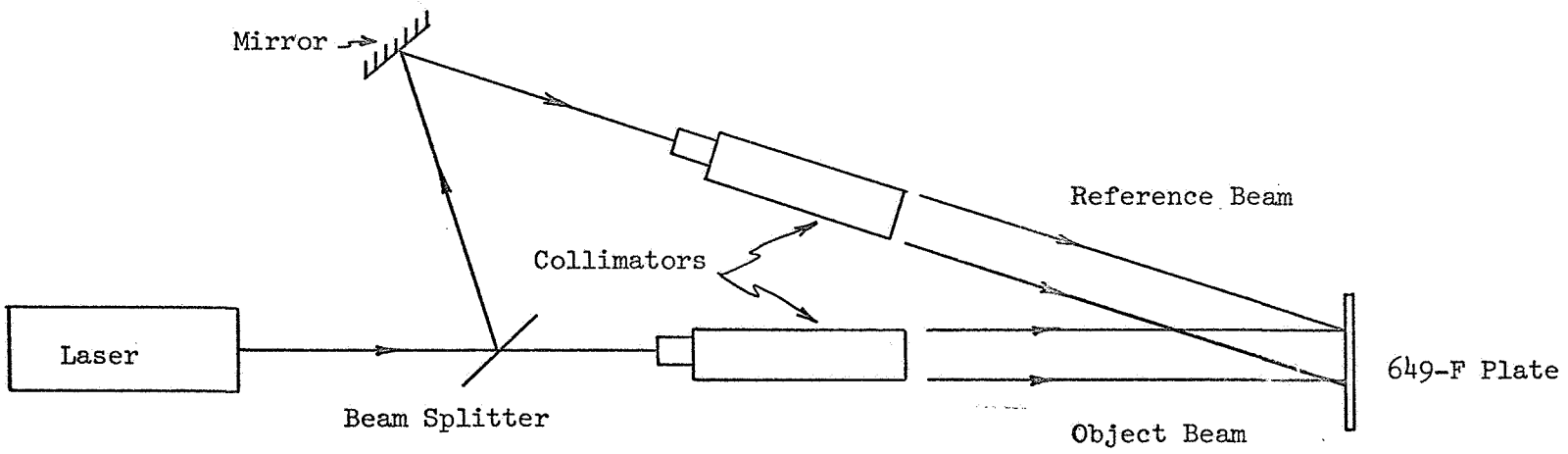

Figure 19

TYPICAL HOLOGRAM RECORDING ARRANGEMENT WHICH CAN BE USED
TO PRODUCE DUAL EXPOSURE HOLOGRAPHIC INTERFEROGRAMS

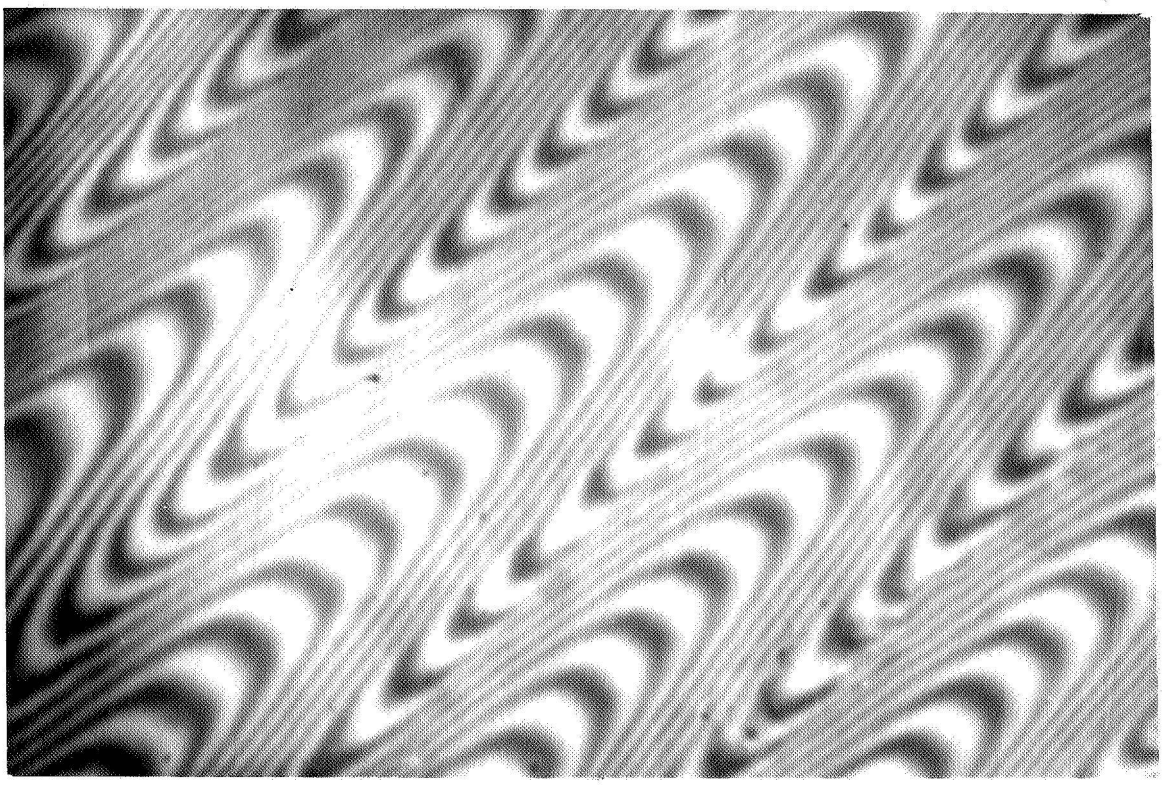

Figure 20

FINITE FRINGE INTERFERENCE PATTERN SHOWING EMULSION RELIEF

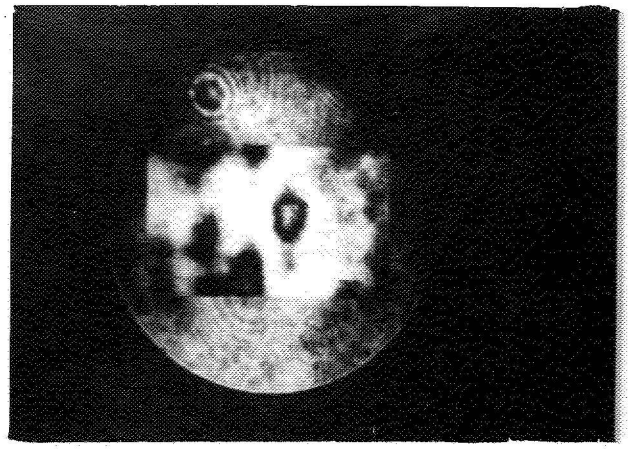

Figure 22

RECONSTRUCTION OF DUAL EXPOSURE
HOLOGRAPHIC INTERFEROGRAM OF WASH-OFF
RELIEF KODAK HIGH CONTRAST COPY FILM STRIP

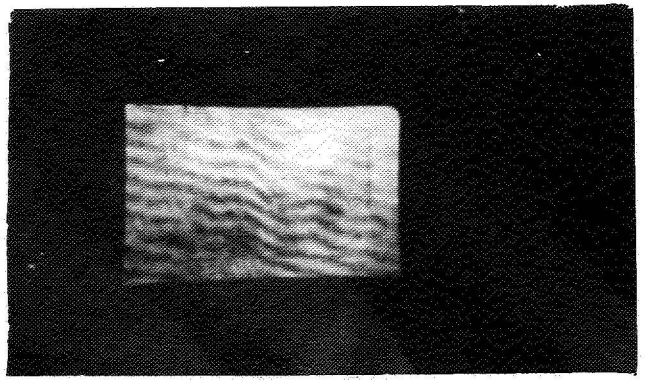

Figure 23

DIFFERENTIAL FINITE FRINGE INTERFEROGRAM SHOWING
ADDITIONAL RELIEF DUE TO THE WASH-OFF STEP ALONE

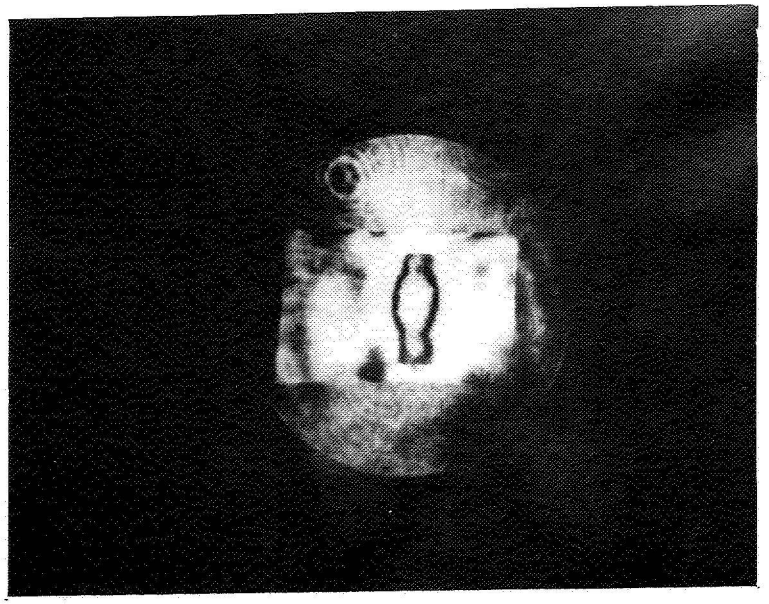

Figure 21

RECONSTRUCTION OF DUAL EXPOSURE HOLOGRAPHIC
INTERFEROGRAM OF BLEACHED KODAK HIGH
CONTRAST COPY FILM STRIP